Zoological Journal of the Linnean Society, 2020, **XX**, 1–39. With 12 figures.

Systematics and historical biogeography of Neotropical foam-nesting frogs of the *Adenomera heyeri* clade (Leptodactylidae), with the description of six new Amazonian species

THIAGO R. D. CARVALHO[1,2*], LEANDRO J. C. L. MORAES[3], ALBERTINA P. LIMA[3], ANTOINE FOUQUET[4], PEDRO L. V. PELOSO[5], DANTE PAVAN[6], LEANDRO O. DRUMMOND[7], MIGUEL T. RODRIGUES[8], ARIOVALDO A. GIARETTA[9], MARCELO GORDO[10], SELVINO NECKEL-OLIVEIRA[11], and CÉLIO F. B. HADDAD[1]

[1]*Laboratório de Herpetologia, Departamento de Biodiversidade, Instituto de Biociências, Universidade Estadual Paulista (UNESP), Rio Claro, 13506-900 SP, Brazil*
[2]*Department of Biological Sciences, University of the Pacific (UOP), Stockton, 95211 CA, USA*
[3]*Coordenação de Biodiversidade, Instituto Nacional de Pesquisas da Amazônia (INPA), Manaus, 69067-375 AM, Brazil*
[4]*Laboratoire Evolution et Diversité Biologique (EDB), CNRS, 31077 Toulouse, France*
[5]*Instituto de Ciências Biológicas, Universidade Federal do Pará (UFPA), Belém, 66075-110 PA, Brazil*
[6]*Ecosfera Consultoria e Pesquisa em Meio Ambiente, Ltda., São Paulo, 05591-120 SP, Brazil*
[7]*Laboratório de Ciências Ambientais, Centro de Biociências e Biotecnologia, Universidade Estadual Norte Fluminense (UENF), Campos dos Goytacazes, 28013-602 RJ, Brazil*
[8]*Departamento de Zoologia, Instituto de Biociências, Universidade de São Paulo (USP), São Paulo, 05508-220 SP, Brazil*
[9]*Laboratório de Taxonomia e Sistemática de Anuros Neotropicais, Instituto de Ciências Exatas e Naturais do Pontal, Universidade Federal de Uberlândia (UFU), Ituiutaba, 38304-402 MG, Brazil*
[10]*Laboratório de Biologia da Conservação and Programa de Pós-Graduação em Zoologia, Instituto de Ciências Biológicas, Universidade Federal do Amazonas (UFAM), Manaus, 69067-005 AM, Brazil*
[11]*Departamento de Ecologia e Zoologia, Universidade Federal de Santa Catarina (UFSC), Florianópolis, 88040-900 SC, Brazil*

Received 22 December 2019; revised 1 April 2020; accepted for publication 14 April 2020

A large proportion of the biodiversity of Amazonia, one of the most diverse rainforest areas in the world, is yet to be formally described. One such case is the Neotropical frog genus *Adenomera*. We here evaluate the species richness and historical biogeography of the *Adenomera heyeri* clade by integrating molecular phylogenetic and species delimitation analyses with morphological and acoustic data. Our results uncovered ten new candidate species with interfluve-associated distributions across Amazonia. In this study, six of these are formally named and described. The new species partly correspond to previously identified candidate lineages 'sp. F' and 'sp. G' and also to previously unreported lineages. Because of their rarity and unequal sampling effort of the *A. heyeri* clade across Amazonia, conservation assessments for the six newly described species are still premature. Regarding the biogeography of the *A. heyeri* clade, our data support a northern Amazonian origin with two independent dispersals into the South American Dry Diagonal. Although riverine barriers have a relevant role as environmental filters by isolating lineages in interfluves, dispersal rather than vicariance must have played a central role in the diversification of this frog clade.

ADDITIONAL KEYWORDS: bioacoustics – biodiversity – Brazil – distribution patterns – diversification – Dry Diagonal – riverine barriers – South America.

*Corresponding author. E-mail: thiago_decarvalho@yahoo.com.br
[Version of record, published online 4 August 2020; http://zoobank.org/ urn:lsid:zoobank.org:pub: 66F0EFA1-25AF-46DE-A7EA-926909CE01EB]

INTRODUCTION

The number of species found in the Neotropics exceeds that of other tropical regions (Qian & Ricklefs, 2007) and the origins of this astonishing diversity have puzzled biologists for over two centuries (e.g. von Humboldt, 1825; Wallace, 1852). Intricate geomorphological and climatic events of the Neogene have been proposed as important causes of the South American megadiversity (Smith *et al.*, 2014; Silva *et al.*, 2019), most notably as a consequence of the uplift of the Andes cordillera during the Miocene–Pliocene [reviewed by Hoorn *et al.* (2010) for Amazonia]. Another striking feature of South American biota is the north-east–south-west belt of open formations (Prado & Gibbs, 1993), the 'Dry Diagonal' (DD: Chaco, Cerrado and Caatinga), which acts as a barrier for biotic exchange between Amazonia and the Atlantic Forest (Costa, 2003; Batalha-Filho *et al.*, 2013).

Amazonia has certainly played a central role in Neotropical diversification, providing more lineages than receiving from other biogeographic regions (Antonelli *et al.*, 2018). Nevertheless, the timing and intensity of these exchanges remain poorly documented between Amazonia and the DD, especially for amphibians [see de Sá *et al.* (2019) for an example]. Moreover, the evolutionary processes of diversification within Amazonia remain poorly understood. The historical and contemporary configuration of riverine networks in Amazonia has been widely associated with distribution patterns of many vertebrate groups (Haffer, 1978; Cracraft, 1985; Azevedo-Ramos & Galatti, 2002; Silva *et al.*, 2012; Naka & Brumfield, 2018). However, the river-barrier hypothesis does not apply universally, and other historical geological events and environmental factors, such as marine incursions, ancient structural arches, climatic conditions and geographic distance, also have important contributions for current species distributions throughout Amazonia (Leite & Rogers, 2013; Smith *et al.*, 2014; Dagosta & de Pinna, 2017; Fluck *et al.*, 2020).

PHYLOGENY AND SPECIES RICHNESS IN *ADENOMERA* FROGS

Species richness in the terrestrial foam-nesting frogs of the genus *Adenomera* Steindachner, 1867 is certainly highly underestimated throughout South America (e.g. Angulo *et al.*, 2003; Kwet, 2007; Carvalho & Giaretta, 2013a, b). Fouquet *et al.* (2014) published a comprehensive phylogenetic study of *Adenomera* frogs based on molecular data and showed that the number of species is underestimated in more than 50% relative to its currently recognized species content. In the same study, members of the genus were classified into eight major clades. One of these, the *A. heyeri* clade, was recovered as being comprised of one nominal species distributed in the Guiana Shield [*A. heyeri* (Boistel *et al.*, 2006)] and unnamed genetic lineages (i.e. confirmed candidate species) distributed across most of Amazonia and the central north-eastern portion of the DD. The *A. heyeri* clade constitutes a group of species that have diversified at the interface between major biogeographic regions of forest and open-formation environments in South America and therefore it is well-suited for further investigation of its systematics, species richness and biogeographic history. The *A. heyeri* clade comprises the nominal species and five additional new candidate species [i.e. the lineages 'sp. F', 'sp. G', 'sp. H', 'sp. I' and 'sp. Q'; *sensu* Fouquet *et al.* (2014)]. However, the available phenotypic data for this clade are still exiguous. Recently, a new species of the *A. heyeri* clade was described and assigned to the Amazonian lineage sp. F: *Adenomera phonotriccus* Carvalho, Giaretta, Angulo, Haddad & Peloso, 2019. That taxonomic study confirmed that even major lineages previously indicated as confirmed candidate species by Fouquet *et al.* (2014) harbour additional cryptic species complexes, given that *A. phonotriccus* (=clade F3) is conspecific only with one of three clades within sp. F (clades F1–F3).

In this review, we evaluate the species richness of the *A. heyeri* clade based on the congruence of reciprocal monophyly across mitochondrial and nuclear gene datasets and molecular-based species delimitation analysis with divergence in phenotypic characters (i.e. morphology, coloration and calls). The main results of this integrative study are: (1) the discovery of ten new candidate species, of which six are described herein as new; (2) the first association of *Adenomera cotuba* Carvalho & Giaretta, 2013 and *Adenomera juikitam* Carvalho & Giaretta, 2013 to two of the previously recognized confirmed candidate species of Fouquet *et al.* (2014) based on new DNA sequence data from their type series; and (3) updated diagnoses for *A. cotuba*, *A. heyeri* and *A. juikitam*. Our phylogenetic and species delimitation analyses provide a suitable framework for the investigation of the historical biogeography of the *A. heyeri* clade using comprehensive geographical sampling across Amazonia and the DD. From this perspective, we sought to elucidate the relative role of riverine barriers in the diversification of this frog clade in a scenario of allopatric and sympatric distributions associated with interfluves across the southern Amazon Basin and north of the main course of the Amazon River.

MATERIAL AND METHODS

COLLECTION DATA AND INSTITUTIONAL ACRONYMS

Field data were collected by us during the last decade from several expeditions to distinct Amazonian regions

(see Figs 1–2). Detailed information on localities can be found in the taxonomic accounts. Institutional acronyms follow Sabaj (2019), except the museums and collections that are not included there, abbreviations are CZPB-AA (Coleção Zoológica Paulo Bührnheim, Universidade Federal do Amazonas, in Manaus, Amazonas), LHUFCG (Herpetological collection of the Universidade Federal de Campina Grande, in Patos, Paraíba) and AF (Antoine Fouquet's field series). A list of morphologically examined specimens of *Adenomera* can be found in Supporting Information (Appendix S1).

Acquisition and analysis of DNA sequence data

We compiled a molecular dataset for the genus *Adenomera* based on new sequences produced for this study and sequences from the GenBank online repository (Clark *et al.*, 2016), which integrated the most recent phylogeny of the genus (Fouquet *et al.*, 2014) and those published by Carvalho *et al.* (2019c). Taxon sampling included nominal *A. heyeri* and all available genetic data of lineages in the *A. heyeri* clade, in addition to each operational taxonomic unit (OTU) of nominal species from the other seven *Adenomera* clades delimited by Fouquet *et al.* (2014). This dataset with 178 individuals comprises four mitochondrial genes (coverage in the completed dataset): the 12S (21%) and 16S (23%) RNAs, and the coding genes cytochrome oxidase I—*COI* (100%) and cytochrome *b*—*Cytb* (72%), plus four nuclear genes: recombination activating gene exon 1—*Rag1* (72%), pro-opiomelanocortin C—*POMC* (72%), tyrosinase—*TYR* (21%) and rhodopsin—*Rhod* (21%). Genomic DNA of new samples was extracted from tissue samples stored in 100% ethanol following the protocols of the Wizard® Extraction Kit (Promega, Madison, WI) or using standard ammonium precipitation method (Lyra *et al.*, 2017). The sister group of *Adenomera*, *Lithodytes lineatus* (Schneider, 1799) and species from related genera (*Hydrolaetare* Gallardo, 1963 and *Leptodactylus* Fitzinger, 1826) were selected as outgroups for the analysis. We amplified *COI* fragments using primers dgLCO1490/dgHCO2198 (Meyer, 2003) and T3–AnF1/T7–AnR1 (Lyra *et al.*, 2017), as well as 16S fragments for some specimens using primers 16Sar/16Sbr (Palumbi *et al.*, 1991). DNA amplification and purification follow the methods of Lyra *et al.* (2017). Products of PCR were sequenced at Macrogen, Inc. (Seoul, South Korea) with a BigDye Terminator Cycle Sequencing Kit (v.3.0; Applied Biosystems, Waltham, USA) in an ABI 3730 automated DNA sequencer (Applied Biosystems, Waltham, USA). Accession numbers and associated information for GenBank and new sequences can be found in Supporting Information (Appendix S2).

We edited new sequences using Geneious v.8 (Kearse *et al.*, 2012). Each gene was independently aligned using the MAFFT v.7 online (Katoh & Standley, 2013) under default parameters, except by the use of the E-INS-i strategy for the RNAs, due to multiple conserved domains and long gaps, and the G-INS-i strategy for remaining genes, because of sequences with global homology (Katoh & Standley, 2013). All genes were posteriorly concatenated using Geneious, leading to a final 6423 bp alignment. We used the concatenated dataset for downstream phylogenetic analyses, as preliminary analyses of individual gene trees showed low resolution for the deepest nodes. We inferred the phylogeny through a Bayesian phylogenetic framework using this complete dataset (all genes, 178 individuals + 3 outgroups) in MrBayes v.3.2.6 (Ronquist *et al.*, 2012), using four independent runs of 10^7 generations. The GTR+I+G was the best-fitting substitution model to all four partitions (RNAs + each codon of remaining genes), according to a BIC (Bayesian Information Criterion) estimate with PartitionFinder v.2.1.1 (Lanfear *et al.*, 2017). We assessed convergence of parameters (Estimated Sample Size, ESS > 200) using Tracer v.1.7 (Rambaut *et al.*, 2018) and discarded a 10% burn-in of samples.

Within the *A. heyeri* clade, we focused on the *COI* gene (sampled for all individuals) to calculate the uncorrected pairwise genetic distances (Table 1), removing gaps through pairwise deletion with MEGA v.7 (Kumar *et al.*, 2016). The intra- vs. interspecific threshold of genetic distances was defined as 5% based on our results for the diversification of this *Adenomera* clade (Table 1), supported by the previous inferences published for the entire genus (Fouquet *et al.*, 2014). We conducted a species delimitation analysis through the Approximate Barcode Gap Discovery method (ABGD; Puillandre *et al.*, 2012) at the web interface (https://bioinfo.mnhn.fr/abi/public/abgd/abgdweb.html; version '6 March 2020') using a prior of intraspecific divergence (P) between 0.001 and 0.1, a proxy for minimum relative gap width (X) of 1, and a number of bins (N) of 30. The intraspecific divergence was defined as 1%, a threshold recognized in vertebrate species delimitation analyses, and the end of a plateau for number of groups (named OTU), as the 11th partition to delimit OTUs (Puillandre *et al.*, 2012).

After delimiting the OTUs in the *A. heyeri* clade based on the combined analysis of DNA sequence, acoustic and morphological data, we selected one terminal per species for the reconstruction of a Bayesian time-calibrated phylogenetic tree. With a dataset containing 43 samples of *Adenomera*, three outgroups and all available genes, we reconstructed the tree using BEAST v.2.4 (Bouckaert *et al.*, 2014). We used a birth-death model of diversification (Gernhard,

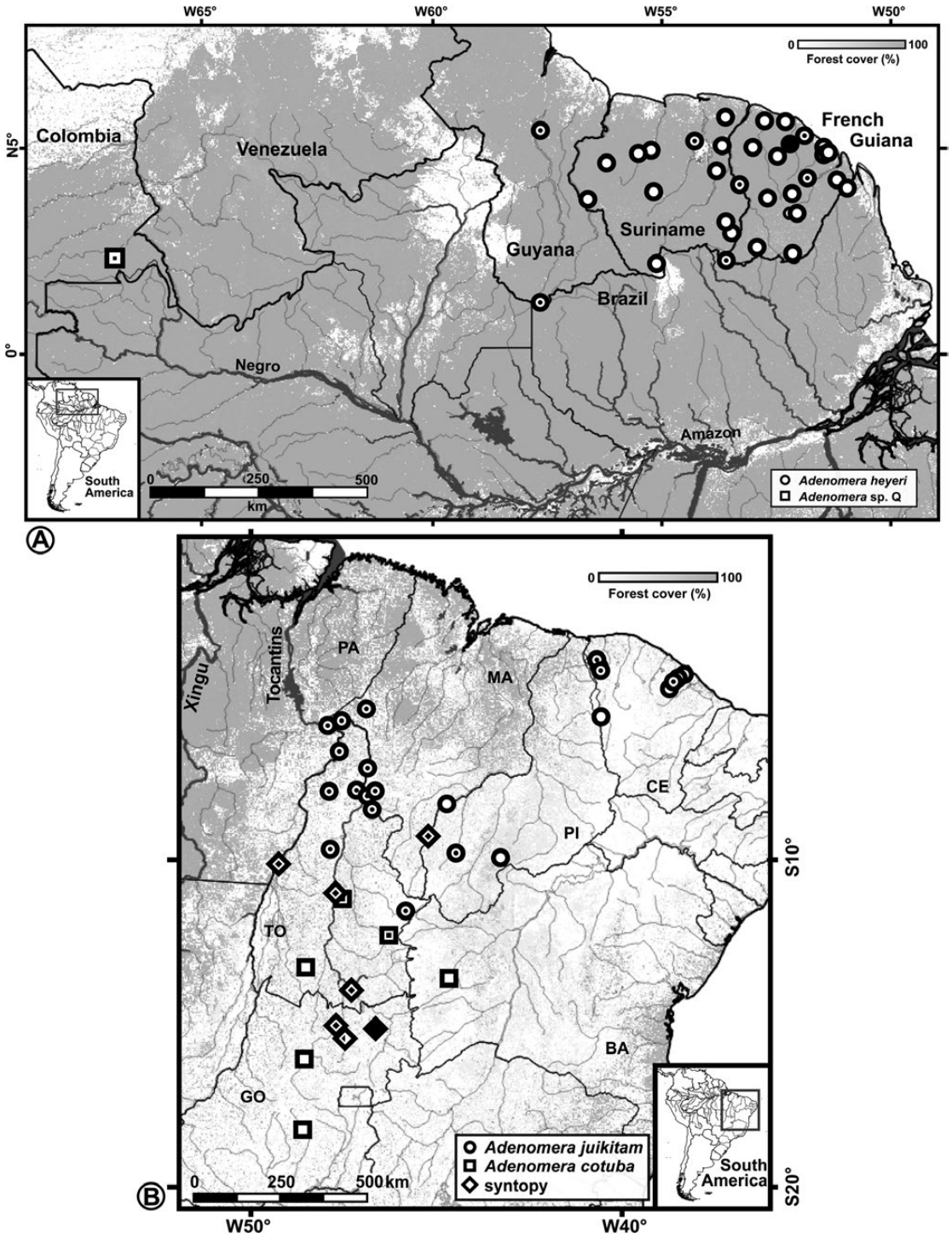

Figure 1. Distribution of lineages of the *A. heyeri* clade associated with (A) northern Amazonia (*A. heyeri* and sp. Q) and (B) the Dry Diagonal and the Cerrado-Amazonia ecotone (*A. cotuba* and *A. juikitam*). Solid-filled symbols represent type localities and black-dotted symbols indicate localities with associated genetic data. Brazilian state abbreviations are as follows: BA (Bahia), CE (Ceará), GO (Goiás), MA (Maranhão), PA (Pará), PI (Piauí) and TO (Tocantins).

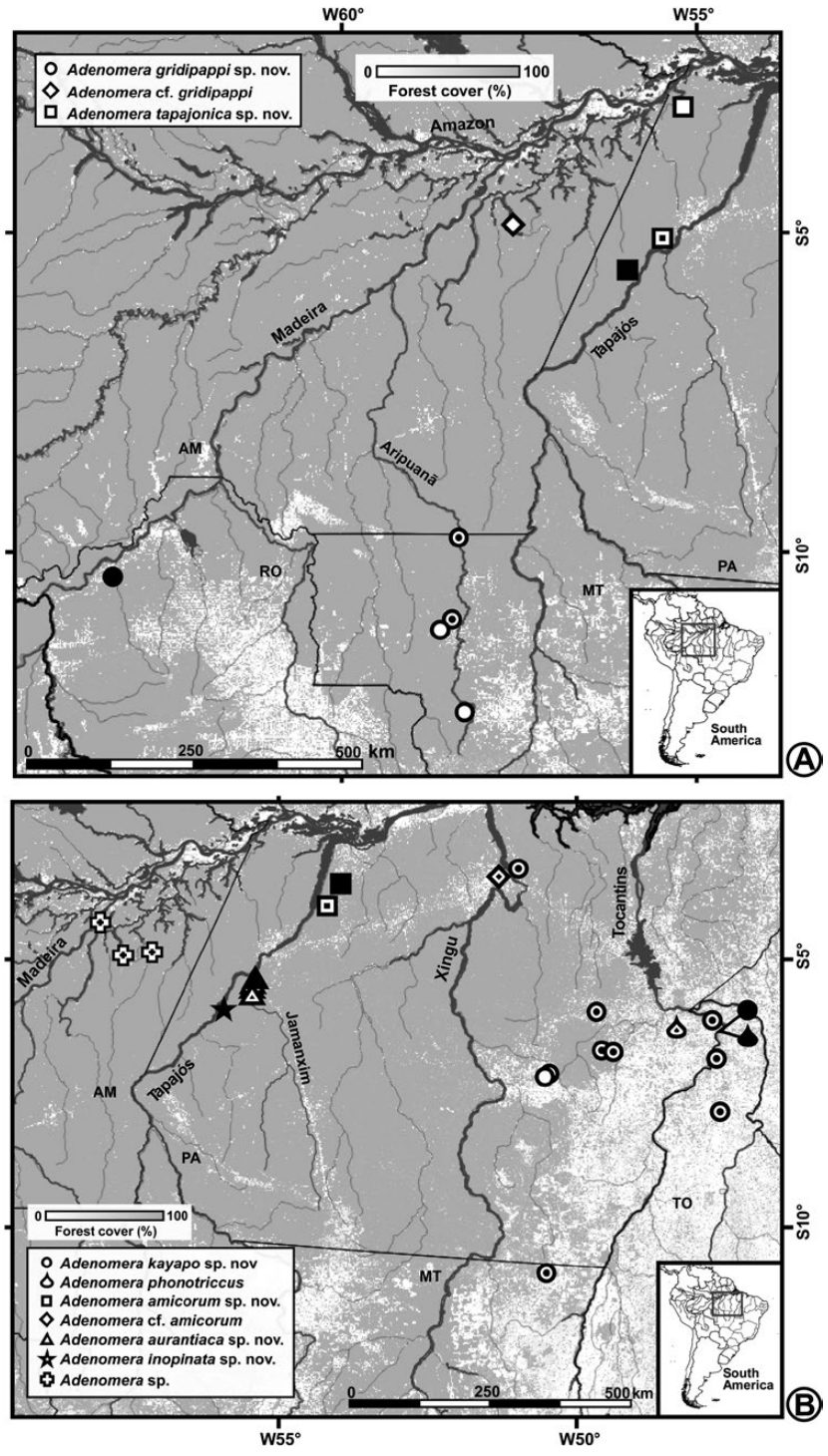

Figure 2. Distribution of lineages of the *A. heyeri* clade associated with the major southern tributaries of the Amazon River (interfluves) and Tocantins River: Madeira-Tapajós (***A. gridipappi***, ***A. tapajonica***, *A.* cf. *gridipappi* and *Adenomera* sp.), Tapajós-Xingu (***A. amicorum***, ***A. aurantiaca***, ***A. inopinata*** and *A.* cf. *amicorum*), Xingu-Tocantins (*A. phonotriccus* and ***A. kayapo***) and Araguaia-Tocantins (***A. kayapo***). Solid-filled symbols represent type localities and black-dotted symbols indicate localities with associated genetic data. Brazilian state abbreviations are as follows: AM (Amazonas), MT (Mato Grosso), PA (Pará), RO (Rondônia) and TO (Tocantins).

Table 1. Mean interspecific (diagonal matrix) and intraspecific (in bold) uncorrected genetic p-distances in *COI* between the 14 Operational Taxonomic Units of the *A. heyeri* clade

	1	2	3	4	5	6	7	8	9	10	11	12	13	14
1. *Adenomera kayapo*	**0.03**													
2. *Adenomera phonotriccus*	0.07	**0.00**												
3. *Adenomera amicorum*	0.08	0.07	**0.00**											
4. *Adenomera* cf. *amicorum*	0.08	0.07	0.05	—										
5. *Adenomera tapajonica*	0.12	0.12	0.12	0.11	**0.04**									
6. *Adenomera gridipappi*	0.13	0.12	0.11	0.12	0.07	**0.00**								
7. *Adenomera* cf. *gridipappi*	0.13	0.12	0.11	0.12	0.08	0.05	**0.01**							
8. *Adenomera* sp.	0.12	0.11	0.11	0.11	0.07	0.08	0.08	**0.03**						
9. *Adenomera aurantiaca*	0.11	0.11	0.11	0.11	0.11	0.10	0.12	0.10	—					
10. *Adenomera inopinata*	0.13	0.12	0.11	0.11	0.11	0.11	0.11	0.10	0.08	—				
11. *Adenomera cotuba*	0.12	0.11	0.10	0.12	0.13	0.12	0.13	0.13	0.13	0.13	**0.02**			
12. *Adenomera heyeri*	0.15	0.15	0.16	0.16	0.17	0.16	0.15	0.16	0.16	0.15	0.16	**0.02**		
13. *Adenomera* sp. Q	0.16	0.17	0.19	0.17	0.17	0.18	0.18	0.18	0.19	0.20	0.18	0.19	—	
14. *Adenomera juikitam*	0.16	0.14	0.15	0.15	0.17	0.16	0.16	0.16	0.16	0.17	0.15	0.15	0.17	**0.04**

2008), an uncorrelated relaxed clock lognormal among branches (Drummond *et al.*, 2006) and calibrated the tree with known ages of two nodes (mean ± standard deviation in Myr): (1) diversification of *Leptodactylus* vs. *Lithodytes* at 36.2 ± 3.2 Mya (Feng *et al.*, 2017); and (2) crown age of *Adenomera* at 25.0 ± 3.0 Mya (Fouquet *et al.*, 2014). Time calibration priors were constrained with a normal distribution. After four parallel runs of MCMC chains with 10^7 iterations, 10^4 of thinning and 10% of burn-in, we combined the log files and assessed the convergence of parameters (ESS > 200) using Tracer, and extracted the maximum clade credibility tree after a burn-in of 25%.

With phylogenetic, spatial and temporal information, we used the package 'BioGeoBears' (Matzke, 2014), implemented in R v.3.5.0 (R Core Team, 2018), to conduct a biogeographic analysis of ancestral area reconstruction of the *A. heyeri* clade. We ran the analysis considering six diversification models: DEC, DIVALIKE, BAYAREALIKE and those including founder-event speciation (+J). Best-fitted models were assessed under the comparison of Akaike Information Criterion corrected for sample size (AICc). Spatial subdivisions followed shared histories, abiotic and biotic affinities of subunits (Cracraft, 1985; Werneck *et al.*, 2012): Amazonia, subdivided by the Amazon River and its largest southern tributaries: the Madeira, Tapajós, Xingu and Tocantins rivers (areas A, B, C and D, respectively), and the South American DD (area E) containing the Cerrado and Caatinga formations. Amazonian subdivisions were based mainly on the historical assessment of biogeographic patterns and processes with respect to shared evolutionary histories of the biota currently delimited by the major rivers in the Amazon Basin (Cracraft, 1985; Ribas *et al.*, 2012; Silva *et al.*, 2019). Although smaller rivers can also be relevant to diversification patterns in Amazonia (Fernandes *et al.*, 2014), our limited spatial sampling within micro-interfluves prevents us from incorporating them into the biogeographic analysis. Using these biogeographic units for the delimitation analysis, we aimed to identify the origin of the *A. heyeri* clade (Amazonia vs. DD), and the main events of vicariance and dispersal in the diversification of this clade. Considering that OTUs within the *A. heyeri* clade were mostly restricted to one of the spatial subdivisions in Amazonia, non-adjacent ancestral distributions were excluded from analysis, and the maximum number of ancestral areas was limited to two.

Morphology and colouration

Adult specimens were examined for morphological and chromatic characteristics. Sexual maturity of examined specimens was determined by the presence of vocal slits and a fleshy ridge at the snout tip in the case of males (besides those collected while calling) and by the presence of eggs visible through the ventral body wall in the case of females. Also, gravid females are markedly more robust than males in *Adenomera*, thus providing indirect evidence that a female can be assessed as an adult individual through body shape. Eleven body measurements were taken from specimens using a stereomicroscope (except for SVL which was measured with callipers) fitted with a micrometric ocular piece (10 mm scale) and are listed as follows: snout–vent length (SVL), thigh length (THL), tibia length (SL), foot length (FL), hand length (HAL), head length (HL), head width (HW), eye diameter (ED), tympanum diameter (TD), eye–nostril distance (EN) and internarial distance (IND). Measurements

mostly follow the definitions of Watters *et al.* (2016). Three measurements (HL, HW and HAL) follow those of Carvalho *et al.* (2019a). Colour patterns were described on the basis of field notes and photographs of individuals in life. Snout shapes were assessed according to Heyer *et al.* (1990). Toe tip development (character states A–D) was assessed according to Heyer (1973), modified by Carvalho *et al.* (2019d).

Unless otherwise stated, comparisons of morphological and chromatic characters among species of *Adenomera* throughout the taxonomic accounts were based primarily on specimens examined and measured for this study (Table 2; Supporting Information, Appendix S1) and the following studies [when applicable, taxonomic authorities in square brackets]: *Adenomera ajurauna* [Berneck, Costa & Garcia, 2008] (Berneck *et al.*, 2008), *Adenomera andreae* [Müller, 1923] (Carvalho *et al.*, 2019d), *Adenomera araucaria* Kwet & Angulo, 2002 (Carvalho *et al.*, 2019b), *Adenomera bokermanni* [Heyer, 1973] (Carvalho *et al.*, 2019b), *Adenomera chicomendesi* Carvalho, Angulo, Kokubum, Barrera, Souza, Haddad & Giaretta, 2019 (Carvalho *et al.*, 2019a), *Adenomera coca* [Angulo & Reichle, 2008] (Angulo & Reichle, 2008), *Adenomera cotuba* (Carvalho & Giaretta, 2013a), *Adenomera diptyx* [Boettger, 1885] (Carvalho & Giaretta, 2013b), *Adenomera engelsi* Kwet, Steiner & Zillikens, 2009 (Carvalho *et al.*, 2019a, c), *A. heyeri* (Boistel *et al.*, 2006), *Adenomera hylaedactyla* [Cope, 1868] (Carvalho *et al.*, 2019d), *Adenomera juikitam* (Carvalho & Giaretta, 2013a), *Adenomera kweti* Carvalho, Cassini, Taucce & Haddad, 2019 (Carvalho *et al.*, 2019b), *Adenomera lutzi* Heyer, 1975 (Kok *et al.*, 2007), *Adenomera marmorata* Steindachner, 1867 (Cassini *et al.*, 2020), *Adenomera martinezi* [Bokermann, 1956] (Carvalho & Giaretta, 2013b), *Adenomera nana* [Müller, 1922] (Carvalho *et al.*, 2019b), *Adenomera phonotriccus* (Carvalho *et al.*, 2019c), *Adenomera saci* Carvalho & Giaretta, 2013 (Carvalho & Giaretta, 2013b), *Adenomera simonstuarti* [Angulo & Icochea, 2010] (Angulo & Icochea, 2010) and *Adenomera thomei* [Almeida & Angulo, 2006] (Almeida & Angulo, 2006).

Sound recordings and acoustic analysis

Calls were recorded in the field at 44.1 or 48.0 kHz sampling rates and 16 bit depth, and stored as uncompressed wave files, except for two recordings from Porto Velho (Madeira River), originally stored as MP3 files and converted into wave format for acoustic analysis—this was necessary due to a low sample size of calls from the Madeira River Basin. Comparisons between the acoustic traits quantified between converted files and those originally stored as wave files were self-consistent, thus we decided to keep converted files in the dataset. Additional calls were obtained from the sound guide to frogs of French Guiana (Marty & Gaucher, 1999), the Macaulay Library collection at the Cornell Lab of Ornithology (ML) and the Fonoteca Neotropical Jacques Vielliard (FNJV). Calls were analysed using an interface built between an expanded version (0.9.6.1) of Soundruler (Gridi-Papp, 2007) and Matlab v.6.5.2 (Matlab, 2004). Acoustic traits were quantified through automated analysis. Data are presented in acoustic descriptions as range (mean ± standard deviation). Ranges include the span of values from the raw dataset. In the case of pulse duration and pulse interval, given that acoustic signals analysed had more than one pulse, we first averaged the duration of each pulse of a given note (call mean) and then obtained the averaged mean for each male analysed from the mean duration of call pulses (individual mean), and lastly we obtained the grand means and associated standard deviations by averaging individual means. Overall spectrogram parameters were set as follows: fast Fourier transform (FFT) size = 1024 points, FFT overlap = 90%, window type = Hanning and window contrast = 70%. Acoustic definitions and terminology followed those of Carvalho *et al.* (2019c). Settings for the automated analysis are given along with information on sound recordings in Supporting Information (Appendix S3). Note rate (per minute) was quantified manually in Audacity v.2.1.1 (Audacity Team, 2017). A high-pass band filter of 500 Hz was applied to sound files in Soundruler prior to conducting the acoustic analysis to reduce background noise caused by wind and/or rain. Sound figures were produced using seewave v.2.1.0 (Sueur *et al.*, 2008) and tuneR v.1.3.2 (Ligges *et al.*, 2017), implemented in R v.3.5.0, with the following parameters: FFT size = 256 points, FFT overlap = 90%, window type = Hanning; the intensity of frequency components was indicated by its darkness in a relative 36 dB scale. If not otherwise stated, acoustic comparisons among species of *Adenomera* throughout the taxonomic accounts follow the quantified traits and associated references of Table 3. Call features attributed hereinafter to *A. diptyx* are based on the description published by Márquez *et al.* (1995). The species was referred therein as *A. hylaedactyla* [see Carvalho *et al.* (2019c) for a discussion concerning species identity of Bolivian populations of *Adenomera*].

Integrative taxonomy and species delimitation

We adopted the unified species concept of de Queiroz (2007). Species delimitation was based mostly on the combination of biological (reproductive isolation), phylogenetic (reciprocal monophyly and diagnosis in qualitative traits) and phenetic (diagnosis in quantitative traits) properties [see Table 1 of de Queiroz

Table 2. Measurements (mm) of the type series (adult specimens only) of the six new species of the *A. heyeri* clade. Morphometric traits are defined in *Material and Methods*. Values are presented as $X \pm$ SD (range). N = sample sizes (M = male, F = female). Measurements of the males of ***A. aurantiaca*** and ***A. inopinata*** correspond to their holotypes

	A. kayapo		*A. amicorum*		*A. aurantiaca*		*A. inopinata*	*A. tapajonica*		*A. gridipappi*
	N = 10 (M)	N = 2 (F)	N = 25 (M)	N = 1 (F)	N = 1 (M)	N = 1 (F)	N = 1 (M)	N = 2 (M)	N = 1 (F)	N = 7 (M)
SVL	18.6 ± 1.0 (17.5–21.0)	20.9 ± 1.2 (20.0–21.7)	22.3 ± 0.8 (20.9–24.0)	22.3	20.9	20.9	23.5	24.6 ± 1.4 (23.6–25.6)	24.0	26.5 ± 0.9 (25.4–27.7)
HL	6.0 ± 0.4 (5.6–6.4)	6.4 ± 0.3 (6.1–6.6)	7.0 ± 0.2 (6.6–7.4)	6.9	6.9	6.5	7.6	8.0 ± 0.1 (7.9–8.1)	7.6	8.0 ± 0.4 (7.7–8.5)
HW	7.0 ± 0.4 (6.6–7.9)	7.7 ± 0.3 (7.4–7.9)	8.1 ± 0.3 (7.6–8.7)	8.1	7.6	7.6	9.4	8.9 ± 0.7 (8.4–9.4)	8.9	9.5 ± 0.4 (9.0–10.0)
ED	1.6 ± 0.1 (1.5–1.8)	1.9 ± 0.1 (1.8–1.9)	1.8 ± 0.1 (1.6–2.1)	1.6	1.8	1.9	2.1	2.1	2.1	2.1 ± 0.2 (1.9–2.3)
TD	1.2 ± 0.1 (1.1–1.5)	1.5 ± 0.2 (1.3–1.6)	1.3 ± 0.2 (0.8–1.5)	1.0	1.1	1.3	1.3	1.5	1.5	1.5 ± 0.1 (1.3–1.6)
EN	1.5 ± 0.2 (1.1–1.8)	1.5 ± 0.1 (1.5–1.6)	1.6 ± 0.1 (1.3–1.9)	1.6	1.6	1.6	1.1	1.9 ± 0.1 (1.8–1.9)	2.1	1.9 ± 0.2 (1.8–2.3)
IND	1.6 ± 0.1 (1.5–1.8)	1.9	1.9 ± 0.2 (1.6–2.1)	1.8	1.9	1.9	1.9	2.2 ± 0.1 (2.1–2.3)	2.4	2.4 ± 0.1 (2.3–2.6)
HAL	4.1 ± 0.3 (3.7–4.7)	4.7 ± 0.7 (4.2–5.2)	4.5 ± 0.4 (3.7–5.0)	4.2	4.0	4.4	5.2	5.1 ± 0.3 (4.8–5.3)	5.6	5.4 ± 0.2 (5.0–5.6)
TL	8.2 ± 0.6 (7.7–9.5)	8.7 ± 0.2 (8.5–8.9)	9.2 ± 0.3 (8.7–9.7)	10.2	8.9	10.0	10.5	10.2 ± 0.6 (9.8–10.6)	11.3	12.0 ± 0.5 (11.3–12.6)
THL	7.9 ± 0.6 (7.3–8.9)	8.0 ± 0.1 (7.9–8.1)	9.1 ± 0.4 (8.4–10.3)	9.5	8.2	9.7	9.4	10.2 ± 0.2 (10.0–10.3)	9.7	11.4 ± 0.9 (9.8–12.3)
FL	8.3 ± 0.9 (6.9–9.8)	9.2 ± 0.7 (8.7–9.7)	9.7 ± 0.5 (8.9–10.6)	10.3	10.0	10.2	11.0	10.6 ± 0.3 (10.3–10.8)	11.0	11.9 ± 1.0 (10.5–12.9)

(2007)]. By adopting this rationale as operational criteria to assessing the existence of separately evolving lineages, we consider as species any monophyletic lineage recovered by the phylogenetic analysis that is diagnosable by at least one fixed phenotypic character (i.e. call or morphology), with the assumption that fixed phenotypic differences are evidence for reduced gene flow among populations (e.g. Frost & Hillis, 1990; Frost *et al.*, 1998; Padial *et al.*, 2012).

RESULTS

Phylogenetic relationships and divergence time estimates

A monophyletic *Adenomera* is supported by a high nodal value in our analysis (Supporting Information, Fig. S1), diverging from the sister group *Lithodytes lineatus* at 37.8 (31–44) Mya, during the Eocene (Supporting Information, Fig. S2). The major groups within *Adenomera* (*A. andreae*, *A. heyeri*, *A. hylaedactyla*, *A. lutzi*, *A. marmorata*, *A. martinezi* and *A. thomei* clades), as defined by Fouquet *et al.* (2014), were also recovered as monophyletic (Supporting Information, Fig. S1). An early diverging group in the early Miocene [21.2 (19–24) Mya] is the *A. andreae* clade, sister to all remaining *Adenomera*, followed by a divergence between clades (*hylaedactyla* + *martinezi* + *thomei* + *marmorata*) and (*heyeri* + *lutzi*), at 19.7 (17–22) Mya. This divergence has a lower nodal support due to the unstable position of the *A. lutzi* clade, which switches between this position and as the sister group of the other five clades. The sister clades recovered are *A. hylaedactyla* + *A. martinezi* with a crown age of 14.9 (12–17) Myr, *A. marmorata* + *A. thomei* with a crown age of 14.4 (12–17) Myr and *A. lutzi* + *A. heyeri* with a crown age of 18.1 (15–21) Myr. Diversification of most *Adenomera* clades began in the Miocene, with most recent divergences detected within the *A. heyeri* and *A. marmorata* clades during the Plio-Pleistocene transitional period (Supporting Information, Fig. S2).

The crown age of the *A. heyeri* clade was inferred at 15.8 (13–18) Mya (Supporting Information, Fig. S2). Within the *A. heyeri* clade, *A. juikitam* was recovered as sister of the remaining 13 lineages, which include *A. heyeri* and several additional unnamed lineages indicated by Fouquet *et al.* (2014) and in the present study (Fig. 3). *A. juikitam* and *A. cotuba* were originally described without genetic data associated (Carvalho & Giaretta, 2013a). We assessed their

Table 3. Summary of major advertisement call traits (presented as value ranges) used in the acoustic diagnosis among species of *Adenomera*: temporal organization, TO (single-note, SN vs. multi-note, MN); note duration, ND (given in ms); pulsing, PP (pulsed vs. non-pulsed, N); pulsing type, PT (incomplete, IP vs. complete, CP); peak frequencies (given in kHz) at the fundamental (H1) and second (H2) harmonics. New species are in bold

Species	TO	ND	PP	PT	H1	H2	Reference
A. ajurauna	SN	130–190	N	N	3.72–5.43	—	Berneck *et al.* (2008)
A. amicorum	MN	133–197	4–10	IP	1.96–2.11	3.90–4.22	Present study
A. andreae	SN	41–76	3–10	IP	2.22–2.59	4.24–5.23	Carvalho *et al.* (2019d)
A. araucaria	SN	102–277	4–18	IP	2.10–2.48	4.11–4.93	Carvalho *et al.* (2019b)
A. aurantiaca	MN	112–137	5–7	CP	2.07–2.25	4.10–4.52	Present study
*A. bokermanni**	SN	99–152	N	N	1.79–1.83	3.40–3.57	Kwet (2007)
A. chicomendesi	SN	154–247	22–35	IP	2.01–2.52	3.94–5.06	Carvalho *et al.* (2019a)
A. coca	SN	110–145	10–15	IP	1.69–1.91	3.45–3.75	Angulo & Reichle (2008)
A. cotuba	MN	68–148	7–22	IP	1.49–1.84	3.02–3.91	Present study
A. diptyx†	SN	44–69	Pulsed	IP	2.08–2.46	4.20–4.79	Márquez *et al.* (1995)
A. engelsi	SN	96–163	N	N	~2.00	3.46–4.29	Kwet *et al.* (2009)
A. gridipappi	MN	50–75	2–4	IP	1.82–1.97	3.55–4.03	Present study
A. heyeri	SN	95–156	4–12	IP	1.79–2.03	3.87–4.36	Present study
A. hylaedactyla	SN	41–89	4–10	IP	1.85–2.21	3.68–4.46	Carvalho *et al.* (2019d)
A. inopinata	MN	70–91	4–5	CP	2.11–2.20	3.98–4.08	Present study
A. juikitam	SN	130–243	11–30	IP	1.77–2.31	3.54–4.85	Present study
A. kayapo	SN	116–156	12–16	IP	2.23–2.41	4.57–4.99	Present study
A. kweti	SN	60–84	N	N	2.36–2.71	4.76–5.41	Carvalho *et al.* (2019b)
A. lutzi	SN	41–61	N	N	1.64–1.81	3.27–3.62	Kok *et al.* (2007)
A. marmorata	SN	21–114	N	N	4.03–5.47	—	Cassini *et al.* (2020)
A. martinezi	SN	63–151	15–21	IP	1.88–2.06	3.38–4.13	Carvalho & Giaretta (2013b)
A. nana	SN	67–122	N	N	2.30–2.70	4.62–5.44	Kwet (2007)
A. phonotriccus	SN	213–433	14–26	CP	1.86–2.00	3.64–4.11	Carvalho *et al.* (2019c)
A. saci	SN	90–241	N	N	1.69–2.25	3.38–4.41	Carvalho & Giaretta (2013b)
A. simonstuarti	MN	57–71	3–4	IP	1.81–2.03	3.71–4.05	Angulo & Icochea (2010)
A. tapajonica	SN	66–89	3–5	IP	1.87–2.00	4.05–4.43	Present study
A. thomei	SN	120–210	10–21	IP	2.15–2.81	4.57–5.56	Almeida & Angulo (2006)

*Reported as *Adenomera* sp. 2 from Joinville.
†Reported as *A. hylaedactyla* [see discussion in Carvalho *et al.* (2019d)].

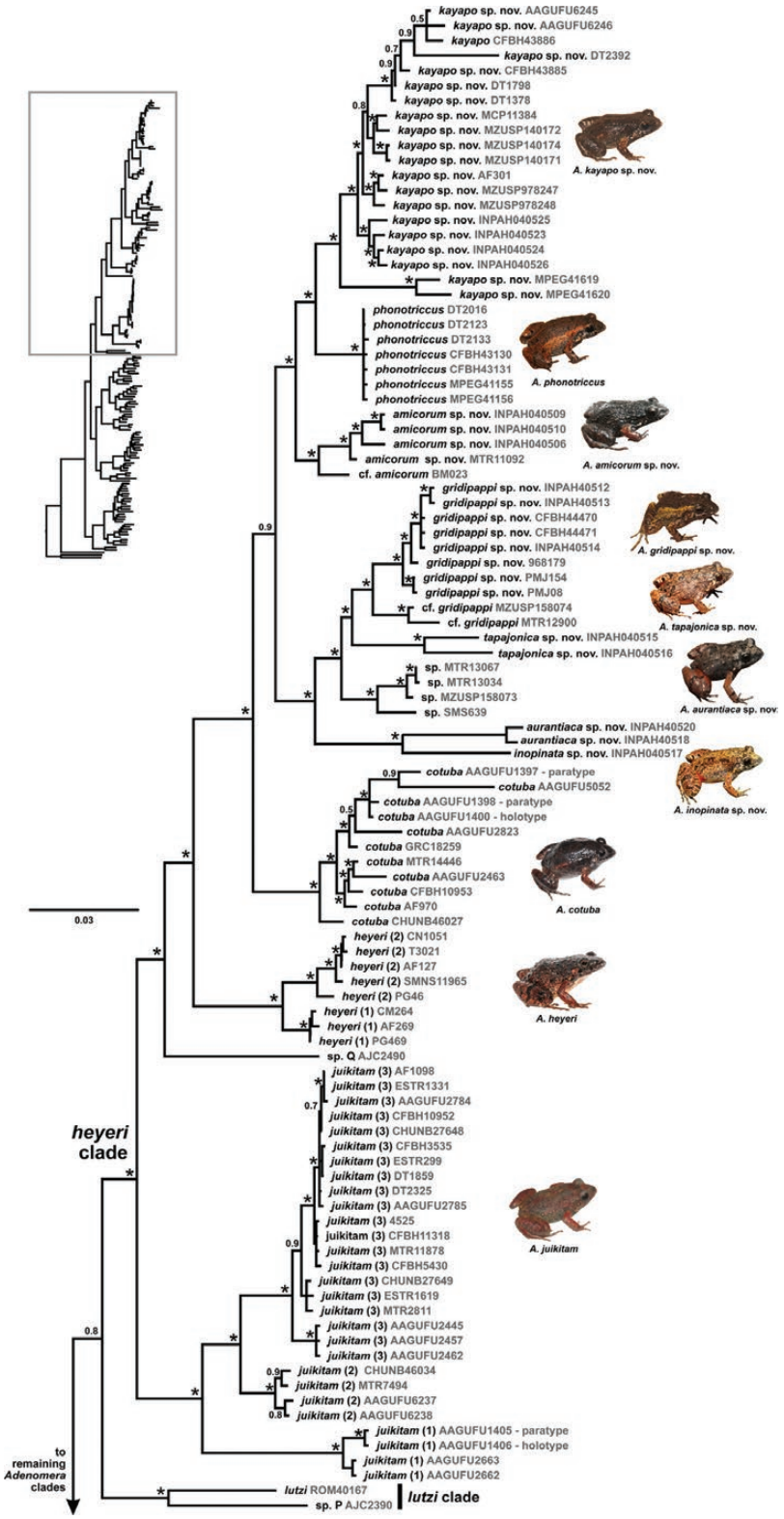

Figure 3. Bayesian phylogenetic tree of *Adenomera* (fully expanded) based on molecular data, focusing on the *A. heyeri* clade and its sister group (A. *lutzi* clade). Numbers near the nodes indicate posterior probabilities (pp) and asterisks indicate full support (pp = 1.0). Branch scale is indicated in number of substitutions per site. See Supporting Information (Fig. S1) for the relationships among *Adenomera* clades.

phylogenetic positions based on type specimens (holotypes and paratypes of both species; see Fig. 3) and non-topotypical specimens. Sequenced individuals of *A. juikitam* and *A. cotuba* were recovered nested, respectively, within the lineages sp. I and sp. H of Fouquet *et al.* (2014). Morphological and acoustic data (detailed in the taxonomy section) support both species as members of the *A. heyeri* clade. The phylogenetic position of *A. cotuba* switches between (i) sister of sp. F or (ii) sister of the sp. F + sp. G clade, and that of sp. Q switches between (i) sister of all taxa except *A. juikitam* and (ii) sister of *A. heyeri*. Such variation had already been noted in previous phylogenetic inferences with essentially the same molecular sampling effort (Fouquet *et al.*, 2014) and might reflect biases on methods, marker origin or extension of missing data, but does not have a relevant effect on the posterior definition of biogeographic units or inferences.

The *A. heyeri* clade as herein defined is composed of four nominal species and several unnamed species. The four named taxa are: *A. heyeri* distributed in the eastern Guiana Shield, *A. juikitam* in the Cerrado, Cerrado-Amazonia ecotone and Caatinga formations (associated, in most cases, with rocky outcrops), *A. cotuba* in the Cerrado savannas and dry forests of north-central Brazil, and *A. phonotriccus* in eastern Amazonia. The remaining unnamed genetic lineages were clustered by Fouquet *et al.* (2014) as sp. F, sp. G and sp. Q. Although sp. F and sp. G are distributed across the major southern tributaries of the Amazon River in Brazilian Amazonia, sp. Q is only known from a single locality, based on a genetic voucher from north-western Amazonia in south-eastern Colombia. Within sp. F and sp. G, the highly structured genetic patterns combined with widespread distribution ranges were found to contain additional cryptic species. The sp. F lineage, subdivided into three subclades [F1, F2, F3 (Fouquet *et al.*, 2014)], was previously studied by Carvalho *et al.* (2019c), leading to the description of *A. phonotriccus* (=F3) and insights into the identity of the other two clades as additional unnamed species. Our analyses recover the same relationship of sp. F and sp. G as sister clades, diverging 8.8 (7–10) Mya. With a broader geographic sampling in our study, we also reveal the existence of three other unnamed lineages from the southern Amazon Basin with affinities to clades within sp. G, which had not been sampled in the previous phylogeny of the genus (Fouquet *et al.*, 2014).

Species delimitation

The molecular-based delimitation analysis indicated 18 OTUs within the *A. heyeri* clade, with four nominal species: *A. juikitam* divided into three subgroups, *A. heyeri* divided into two subgroups, and *A. phonotriccus* and *A. cotuba* as single evolutionary units. The lineage sp. Q of Fouquet *et al.* (2014) and three newly sampled lineages from the Tapajós River region were also recovered as single evolutionary units. Among unnamed lineages, sp. F and sp. G of Fouquet *et al.* (2014) were divided into three and four subgroups, respectively.

Based on the integration of genetic and phenotypic data, we delimited 14 OTUs within the *A. heyeri* clade (Fig. 3). Mean genetic distances between these OTUs range from 5 to 20% (mean 13%) in *COI*, whereas maximum mean distances within OTUs reach 4% (Table 1). Because of the lack of any phenotypic evidence that can support subdivisions within *A. juikitam* and *A. heyeri*, as well as mean *COI* distances below the 5% threshold (Table 1), genetic divergence is regarded as substructuration of single evolutionary units. Five unnamed lineages of Fouquet *et al.* (2014): sp. F2 in part, sp. G1, sp. G2, sp. G4 and sp. Q are treated as unconfirmed candidate species pending the acquisition of acoustic data to address the taxonomic status of these lineages. Two of these (sp. G1 and sp. G4) are regarded as a single evolutionary unit because of the mean *COI* distance below the 5% threshold and geographic co-occurrence. The three remaining lineages (sp. F1, sp. F2 in part and sp. G3) and three newly sampled unnamed lineages were also examined for phenotypic variation, which is consistent with the genetic evidence, and thus warrants their recognition as distinct species.

Biogeographic history

Here we treat as new species the six lineages that are named in the next section of this study 'sp. nov.' of Fig. 4) and as candidate new species those of less certain taxonomic status within the *A. heyeri* clade. Our analysis of reconstruction of ancestral areas recovered the best-fitting model of DIVALIKE+J with log-likelihood = –18.44 (–18.54 for DEC+J, –18.74 for BAYAREALIKE+J, –29.61 for DIVALIKE, –32.50 for DEC and –38.09 for BAYAREALIKE). The origin of the *A. heyeri* clade corresponds most likely to northern Amazonia with the first lineage splitting originating *A. juikitam* via dispersal to the DD during the middle Miocene (Fig. 4). *A. heyeri* and *Adenomera* sp. Q also diverged in northern Amazonia during the middle Miocene. Later in the same geological period a southward dispersal took place from northern Amazonia to the Tapajós-Xingu interfluve. One main clade diversified in this interfluvial region, originating one subclade composed of two new species, and a second subclade that occupied an adjacent interfluvial region (Madeira-Tapajós) during the early Pliocene, composed of two other new species plus two related new candidate species (Fig. 4). The diversification of the second main clade south of the Amazon River includes a second dispersal event to the DD, originating *A. cotuba*, and

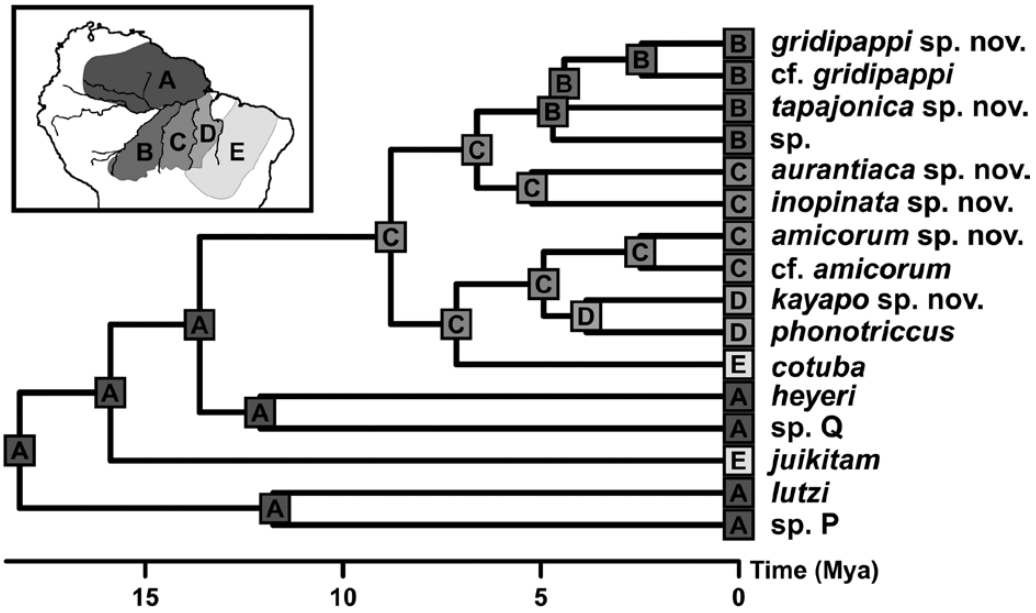

Figure 4. Reconstruction of ancestral areas and diversification of the *A. heyeri* clade and its sister group (A. *lutzi* clade) in Amazonia and the Dry Diagonal (DD), estimated by the DIVALIKE+J model. Letters denote biogeographic units (inset map) as follows: A (northern Amazonia), B (Madeira-Tapajós interfluve), C (Tapajós-Xingu interfluve), D (Xingu-Tocantins interfluve) and E (DD).

the occupation of another interfluvial region (Xingu-Tocantins) and contact zone of Cerrado-Amazonia. This lineage splitting originated a subclade formed by *A. phonotriccus* + one new species, and also an *in situ* origin in the Tapajós-Xingu interfluve of a second subclade formed by another new species + one new candidate species during the late Pliocene (Fig. 4). The overall pattern of diversification within the *A. heyeri* clade likely reflects a series of dispersal events rather than vicariance and can be evidenced as an expansion of diversity in a north–south axis from northern Amazonia to the DD and interfluvial regions south of the Amazon River.

Taxonomy and species descriptions

In this section, we reassess relevant phenotypic data on three species of the *A. heyeri* clade (*A. heyeri*, *A. cotuba* and *A. juikitam*), including updated diagnoses, and describe six of ten candidate species as new based on the congruence of reciprocal monophyly (in both mitochondrial and nuclear DNA) and species delimitation analysis with morphological and acoustic data.

Advertisement call and emended diagnosis of A. heyeri

The call is redescribed based on a larger sample of recordings from French Guiana and Suriname in comparison with the original description (Boistel *et al.*, 2006) and under standardized analytical procedures as a way to enable direct interspecific acoustic comparisons in the next sections. Moreover, the original diagnosis is updated by listing diagnostic traits and highlighting those that are not informative in the current state of *Adenomera* systematics.

The following description is based on calls of five males (N = 42 notes and 327 pulses quantified; Table 3). The advertisement call of *A. heyeri* (Figs 5A, 6A, 7A) consists of a single-note signal given at a low rate of 22–27 (24 ± 2) per minute. Notes are formed by 4–12 (8 ± 2) partly fused pulses given at a rate of 68–89 (80 ± 6) per second, and varying in duration from 5–65 (15 ± 2) ms. Note duration varies from 95–156 (122 ± 22) ms, and note rise time from 18–67 (43 ± 13)% of note duration. The note frequencies are harmonically structured and the dominant frequency may coincide either with the fundamental harmonic (1787–2003 Hz, 1817 ± 57; N = 1 male) or second harmonic (3867–4359 Hz, 4107 ± 232; N = 4 males). Frequency modulation is upward, slight or pronounced, rising to 215–1219 (753 ± 295) Hz.

A. heyeri was originally characterized by the following morphological and colour features and call traits (*sensu* Boistel *et al.*, 2006): (1) two pairs of dorsolateral folds; (2) smooth skin on the sole of foot or with a few small white tubercles; (3) throat and belly yellow in males; and (4) tarsal fold present and slightly marked. Acoustic traits used in the comparisons were: (1) presence of linear and sinusoidal frequency

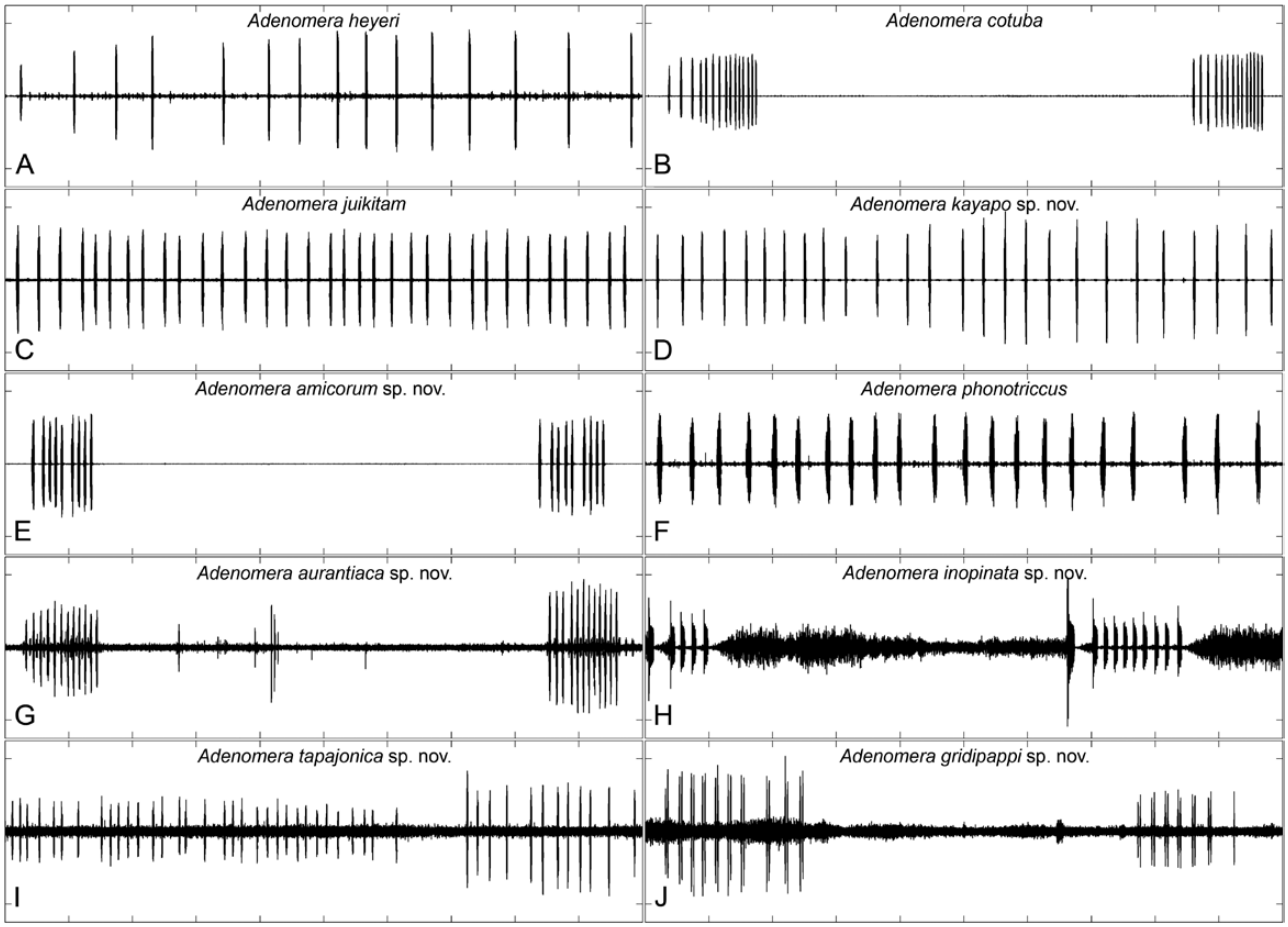

Figure 5. Oscillograms of the temporal organization (single-note vs. multi-note) of advertisement calls in the *A. heyeri* clade. Call sections are equally scaled (40–50 s along the *x*-axis, except in H, for which we produced the figure based on the only available 13-s long sound recording). A, A. *heyeri* from French Guiana, northeastern Amazonia. B, A. *cotuba* from the central Brazilian Cerrado. C, A. *juikitam* from the central Brazilian Cerrado. D, A. *kayapo* from the left bank of the lower Araguaia River, southeastern Amazonia. E, A. *amicorum* from the right bank of the lower Tapajós River, southeastern Amazonia. F, A. *phonotriccus* from the left bank of the lower Araguaia River, southeastern Amazonia. G, A. *aurantiaca* from the right bank of the middle Tapajós River, southeastern Amazonia. H, A. *inopinata* from the right bank of the middle Tapajós River, southeastern Amazonia. I, A. *tapajonica* from the left bank of the middle Tapajós River, southeastern Amazonia. J, A. *gridipappi* from the right bank of the upper Madeira River, southwestern Amazonia. Single-note calls given continuously in A, C–D, F and I; two multi-note calls in B, E, G–H and J. See Appendix S3 for detailed information.

modulations; (2) absence of amplitude modulation and pulses; and (3) dominant frequency coinciding with the second harmonic. Morphological characters #1–2 and #4 are highly variable among members of the genus and as such should preferably not be used as diagnostic eatures. On the other hand, the colour character #3 (ventral surfaces golden yellow in life) is informative for species discrimination within *Adenomera*, given that most species have ventral coloration varying from off-white to cream-coloured.

In addition to a yellow ventral coloration [diagnostic feature #3 of Boistel *et al.* (2006)], the following combination of character states is useful for the diagnosis of *A. heyeri* in the genus *Adenomera*: (1) antebrachial tubercle on underside of forearm absent; (2) nearly solid dark-coloured stripe on underside of forearm absent; (3) toe tips fully expanded into small discs (character state D); (4) single-note advertisement call; (5) call note formed by partly fused pulses; and (6) notes given at a low repetition rate of 22–27 per minute. It is noteworthy that, based solely on yellow ventral coloration (Fig. 8B), *A. heyeri* can be distinguished from most congeners, except the Amazonian *A. chicomendesi* and *A. lutzi*, and the allopatric Atlantic Forest species (*A. araucaria*, *A. bokermanni*, *A. kweti* and *A. nana*). *A. heyeri* differs from *A. lutzi*, *A. cotuba* and *A. phonotriccus* by lacking an antebrachial tubercle on the underside of the forearm. *A. heyeri*

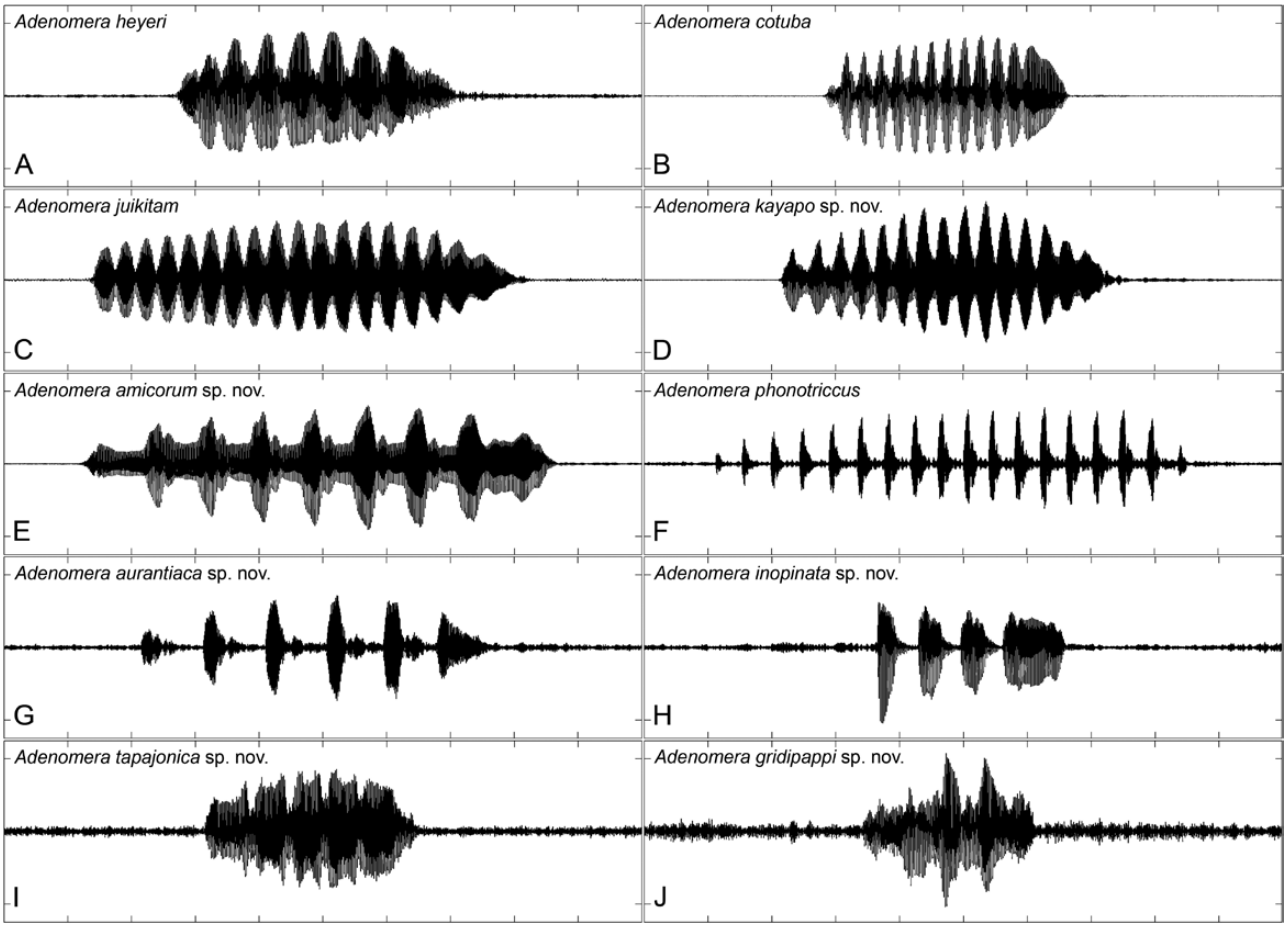

Figure 6. Oscillograms showing the amplitude envelope (incomplete vs. complete pulsing) of advertisement call notes in the *A. heyeri* clade. A, A. *heyeri* from French Guiana, northeastern Amazonia. B, A. *cotuba* from the central Brazilian Cerrado. C, A. *juikitam* from the central Brazilian Cerrado. D, A. *kayapo* from the left bank of the lower Araguaia River, southeastern Amazonia. E, A. *amicorum* from the right bank of the lower Tapajós River, southeastern Amazonia. F, A. *phonotriccus* from the left bank of the lower Araguaia River, southeastern Amazonia. G, A. *aurantiaca* from the right bank of the middle Tapajós River, southeastern Amazonia. H, A. *inopinata* from the right bank of the middle Tapajós River, southeastern Amazonia. I, A. *tapajonica* from the left bank of the middle Tapajós River, southeastern Amazonia. J, A. *gridipappi* from the right bank of the upper Madeira River, southwestern Amazonia. Call sections are equally scaled (c. 250 ms along the *x*-axis, except in F, produced on a 450-ms time scale). Incomplete pulses in A–E and I–J; complete pulses in F–H. See Appendix S3 for detailed information.

has fully expanded toe tips (Fig. 8A–B), differing from most congeners, except *A. ajurauna*, *A. andreae*, *A. chicomendesi*, *A. lutzi*, *A. marmorata*, *A. nana* and *A. simonstuarti*. Regarding call features, the pulsed call of *A. heyeri* differs from the non-pulsed calls of *A. lutzi* and most Atlantic Forest species (Table 3). The single-note call of *A. heyeri* (Fig. 5A) differs from the multi-note call of *A. cotuba* (Fig. 5B) and *A. simonstuarti* (T.R. de Carvalho, pers. obs.); the call note of *A. heyeri* is formed by partly fused pulses (Figs 6A, 7A), whereas that of *A. phonotriccus* is formed by complete pulses (Figs 6F, 7F). The low note repetition rate of *A. heyeri* (22–27 notes/min) differs clearly from the fast-rated notes of the open-habitat species *A. diptyx*, *A. hylaedactyla*, *A. martinezi* and *A. saci* [combined repetition rate of 90–242 notes/min (Márquez *et al.*, 1995; Carvalho & Giaretta, 2013b; Carvalho *et al.*, 2019d)]. The note duration of *A. heyeri* (95–156 ms) differs from those of *A. andreae* [41–76 ms (Carvalho *et al.*, 2019d)] and *A. chicomendesi* [154–247 ms (Carvalho *et al.*, 2019a)].

Distribution and variation in A. cotuba *and* A. juikitam

These species were reported in the literature only three times since their original description

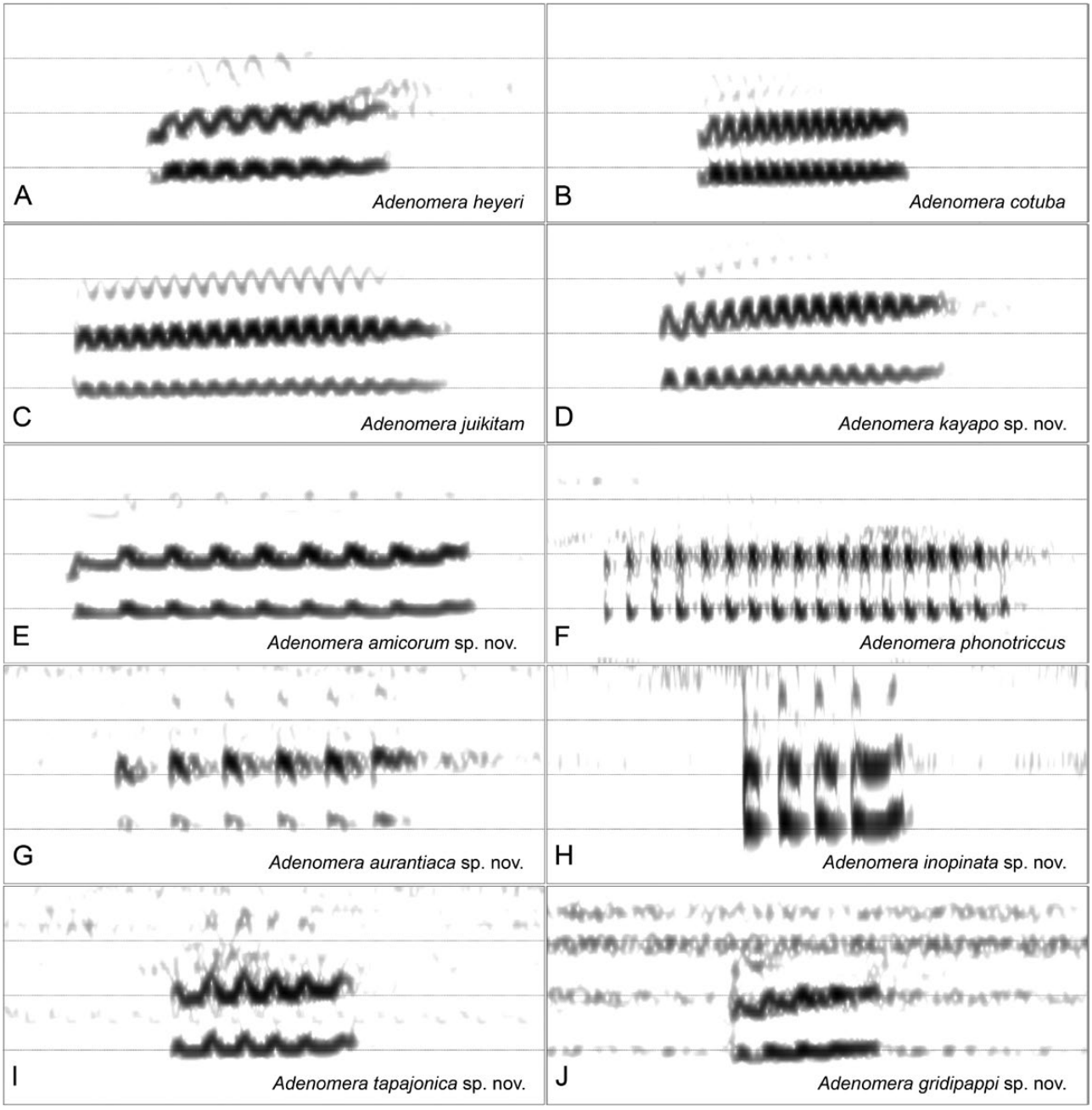

Figure 7. Spectrograms showing the frequency components (sound energy distributed across the first three harmonics) of advertisement call notes in the *A. heyeri* clade. A, A. *heyeri* from French Guiana, northeastern Amazonia. B, A. *cotuba* from the central Brazilian Cerrado. C, A. *juikitam* from the central Brazilian Cerrado. D, A. *kayapo* from the left bank of the lower Araguaia River, southeastern Amazonia. E, A. *amicorum* from the right bank of the lower Tapajós River, southeastern Amazonia. F, A. *phonotriccus* from the left bank of the lower Araguaia River, southeastern Amazonia. G, A. *aurantiaca* from the right bank of the middle Tapajós River, southeastern Amazonia. H, A. *inopinata* from the right bank of the middle Tapajós River, southeastern Amazonia. I, A. *tapajonica* from the left bank of the middle Tapajós River, southeastern Amazonia. J, A. *gridipappi* from the right bank of the upper Madeira River, southwestern Amazonia. Call sections are equally scaled (c. 250 ms along the *x*-axis, except in F, produced on a 450-ms time scale; and at an 8-kHz frequency scale along the *y*-axis). See Appendix S3 for detailed information.

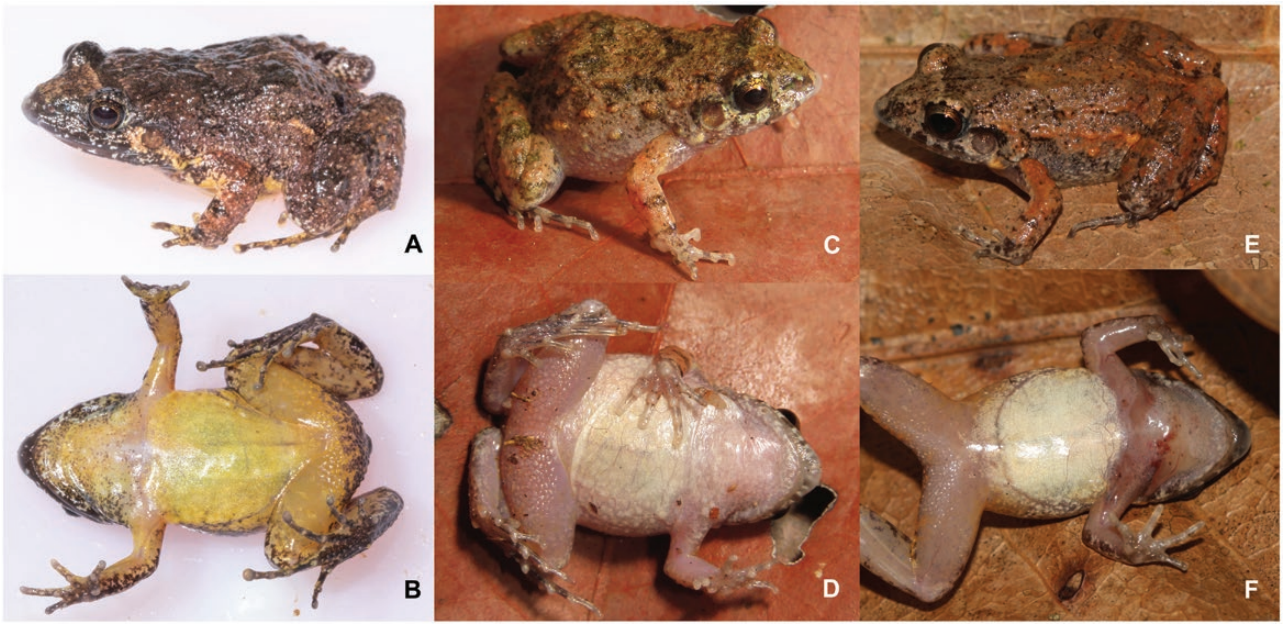

Figure 8. Life colours (adult males) of three species of the *A. heyeri* clade. A–B, *A. heyeri* (AF 2683: SVL not assessed) from Aikéné, in French Guiana. C–D, *A. cotuba* (ZUFMS-AMP 12961: SVL = 21.3 mm) from the District of Taquaruçu (in Palmas), in the Brazilian state of Tocantins. E–F, *A. juikitam* (AAG-UFU 6238: SVL = 18.9 mm) from Aragominas, in the Brazilian state of Tocantins. Photographs of *A. cotuba* by Leandro A. da Silva.

(Carvalho & Giaretta, 2013a). The distribution of *A. cotuba* was extended to São Desidério in western Bahia, north-eastern Brazil (Oliveira *et al.*, 2018), a region without genetic sampling for the species. We recorded and collected three specimens from the same locality (Supporting Information, Appendices S1, S3). Morphological and acoustic data confirm the taxonomic identity of that population as pertaining to *A. cotuba*. With regard to *A. juikitam*, the only report in the Brazilian state of Ceará, north-eastern Brazil (Roberto & Loebmann, 2016), is within the distribution range of the species (reported as sp. I by Fouquet *et al.*, 2014). The most recent report indicates the occurrence of both *A. cotuba* and *A. juikitam* in a few localities in the Brazilian state of Tocantins (Silva *et al.*, 2020). The occurrence areas in Tocantins are consistent with the distribution range of both species based on molecular sampling (Supporting Information, Appendix S2) and examination of specimens and call analysis (Supporting Information, Appendices S1, S3).

Morphological features of additional populations assigned to *A. cotuba* and *A. juikitam* largely agree with the original description (Carvalho & Giaretta, 2013a; Fig. 8C–F). Exceptions are: (1) SVL range of adult males: specimens of other populations attain larger sizes (SVL = 20.6–22.8 mm in *A. cotuba*; SVL = 18.9–23.7 mm in *A. juikitam*) in comparison with type specimens (SVL = 18.6–20.5 mm in *A. cotuba*; SVL = 19.1–19.5 mm in *A. juikitam*); (2) dorsal skin texture: extremely glandular at the type locality, but specimens collected from other localities may have smoother dorsal surfaces; (3) dorsal coloration: the type series of *A. cotuba* was described as nearly solid dark-coloured, but some specimens collected outside the type locality had lighter shades (e.g. marbled pattern) on the dorsum (Fig. 8C). *A. juikitam* was described as having a reddish, marble-like dorsal colouration, which varies to relatively more homogeneous and paler tints in other localities (Fig. 8E). These three features should be used with caution in the identification of specimens of both species, preferably combined with other traits listed in their original diagnoses (Carvalho & Giaretta, 2013a). Calls (Figs 5B–C, 6B–C, 7B–C) recorded from other regions (thirteen males of each of the two species; *A. cotuba*: N = 731 notes and 8363 pulses quantified; *A. juikitam*: N = 400 notes and 7296 pulses quantified; see Appendix S3) also revealed higher intraspecific variation in quantitative acoustic data than previously reported in their original descriptions [Table 3 (Carvalho & Giaretta, 2013a: tables 2, 3)].

New data on females of both species were obtained for the first time. Females are relatively larger compared to males: SVL = 22.1–23.4 mm in *A. cotuba* (N = 2); SVL = 22.0–25.4 mm in *A. juikitam* (N = 3). Other phenotypic traits in females generally agree with those described for male specimens,

except snout shape, which is more rounded both in dorsal and lateral views (males generally have snout subovoid and acuminate in dorsal and lateral views, respectively). Phenotypic traits used in the diagnosis and interspecific comparisons of *A. cotuba* and *A. juikitam* in the next sections take into consideration the new intraspecific variation (morphology and calls) mentioned earlier.

SPECIES DESCRIPTIONS

ADENOMERA KAYAPO, SP. NOV.

KAYAPÓ TERRESTRIAL NEST-BUILDING FROG

(FIGS 2B, 3–4, 5D, 6D, 7D, 9A–B, 11A–B; TABLES 1-3)

lsid urn:lsid:zoobank.org:act:98FCDF08-BD14-46BF-BC3A-0C609EE9887B

Holotype: CFBH 43885 (formerly AAG-UFU 6243; field #TRC 124), adult male, BRAZIL, Pará, Palestina do Pará, 5.701950°S, 48.235240°W, 121 m, 8-i-2018, T.R. de Carvalho, A.A. Giaretta and P. Marinho (Collectors).

Paratypes: CFBH 43886 (formerly AAG-UFU 6244; field #TRC 125) and AAG-UFU 6245–6246 (field #TRC 126–127, respectively), adult males; all with the same collection data as the holotype. MPEG 41619 (field #LOD 1042), adult male, BRAZIL, Pará, Parauapebas, Floresta Nacional (FLONA) de Carajás, 6.076241°S, 50.074451°W, 661 m, 19-i-2018, L.O. Drummond and F.M. Borges (Collectors). MPEG 41620 (field #LOD 1428), adult female, BRAZIL, Pará, Parauapebas, FLONA de Carajás, 6.049913°S, 50.265324°W, 701 m, 23-i-2018, L.O. Drummond and F.M. Borges (Collectors). MPEG 41692 (field #LOD 799), adult male, BRAZIL, Pará, São Félix do Xingu, Serra do Jaguar, Bacia Carapanãzinho, 6.480099°S, 51.249726°W, 236 m, 29-x-2011, L.O. Drummond (Collector). MPEG 41694 (field #LOD 828), adult male, BRAZIL, Pará, São Félix do Xingu, Serra do Jaguar, Bacia Carapanãzinho, 6.456122°S, 51.197732°W, 255 m, 3-xi-2011, L.O. Drummond (Collector). INPA-H 40523–40524, 40526 (field #APL 22299–300, 22302, respectively), adult males, and INPA-H 40525 (field #APL 22301), adult female, BRAZIL, Tocantins, Araguaína, 7.103700°S, 48.197800°W, 227 m, 18-xi-2018, A.P. Lima (Collector).

Referred specimens: Adenomera sp. F, in part (Fouquet *et al.*, 2014: specimens assigned to the lineage F1 in appendices S1a, S3a): MCP 11384 (genetic voucher TG3259), subadult specimen, BRAZIL, Pará, FLONA dos Carajás; MZUSP 140174 (genetic voucher T314), adult male, BRAZIL, Pará, Reserva Biológica (REBIO) Tapirapé.

Additional material: MZUSP 92765, 92784 (adult males) and MZUSP 92774, 92778 (adult females): BRAZIL, Mato Grosso, Vila Rica; MZUSP 140172–73 (adult males; genetic vouchers T220 and T265, respectively): BRAZIL, Pará, REBIO Tapirapé.

Etymology: The name *kayapo* is given as homage to the Kayapó people (sometimes also spelled as Caiapó). The Kayapó is a large group of Jê speaking people living in the south-eastern portion of Brazilian Amazonia. It is thought that the Kayapó, who name themselves *mebêngôkre*, once inhabited a vast region between the Araguaia and Tocantins rivers, but were pushed westward by the early colonizers in the 19th century (Turner, 1998). The Kayapó are known to be fierce protectors of their rights and lands.

Diagnosis: A. kayapo is characterized by the following combination of character states: (1) small size (adult male SVL = 17.5–21.0 mm); (2) robust body shape; (3) toe tips unexpanded or slightly expanded (character states B–C); (4) distal antebrachial tubercle on underside of forearm; (5) two possible chromotypes (presence/absence) of dorsolateral stripe; (6) single-note advertisement call; (7) call note formed by 12–16 partly fused pulses; (8) note duration varying from 116–156 ms; and (9) note dominant frequency coinciding either with the fundamental harmonic (2304 Hz; N = 1 male) or the second harmonic (4570–4992 Hz; N = 3 males).

Comparisons with congeners: A. kayapo has adult males (SVL = 17.5–21.0 mm; Table 2) that are smaller than those (if not otherwise stated, specimens measured are listed in Supporting Information, Appendix S1) of *A. bokermanni* (21.3–22.8 mm), *A. coca* [23.6–25.6 mm (Angulo & Reichle, 2008)], *A. heyeri* [22.5–25.8 mm (Boistel *et al.*, 2006)], *A. hylaedactyla* (21.5–26.5 mm), *A. lutzi* [25.7–33.5 mm (Kok *et al.*, 2007)], *A. martinezi* [21.9–24.2 mm (Carvalho & Giaretta, 2013b)] and *A. simonstuarti* [25.9–26.2 mm (Angulo & Icochea, 2010)]. *A. kayapo* has a robust body shape (Fig. 11A–B), whereas *A. diptyx*, *A. martinezi* and *A. saci* have a slender body (Carvalho & Giaretta, 2013b). *A. kayapo* has unexpanded or slightly expanded toe tips (character states B–C), differing from congeners having toe tips fully expanded into small discs, character state D (*A. ajurauna*, *A. andreae*, *A. chicomendesi*, *A. heyeri*, *A. marmorata*, *A. lutzi*, *A. nana* and *A. simonstuarti*). *A. kayapo* is distinguished from all congeners (except *A. cotuba*, *A. lutzi*, and *A. phonotriccus*) by having an antebrachial tubercle on underside of forearm. *A. kayapo* differs from *A. cotuba*, which does not

have a dorsolateral stripe, by the occurrence of two possible chromotypes (presence/absence) of the stripe. *A. kayapo* and the closest related *A. phonotriccus* are morphologically cryptic species with sympatric distribution (syntopic occurrence at their type locality; Fig. 2B). In contrast, these sister species markedly differ in their advertisement calls.

The advertisement call of *A. kayapo* (Figs 5D, 6D, 7D; Table 3) consists of single notes formed by partly fused pulses. These acoustic characteristics distinguish the new species from the two congeners with multi-note calls, *A. cotuba* (Fig. 5B) and *A. simonstuarti* (T.R. de Carvalho, pers. obs.), and from eight congeners with non-pulsed calls (Table 3). From congeners also having single-note, pulsed calls, *A. kayapo* is distinguished from *A. andreae*, *A. coca*, *A. diptyx*, *A. heyeri*, *A. hylaedactyla* and *A. martinezi* by a longer note duration and/or higher fundamental frequency (Table 3). The call of *A. kayapo* is formed by partly fused pulses (Figs 6D, 7D), whereas that of *A. phonotriccus* is formed by complete pulses (Figs 6F, 7F). The call of *A. kayapo* most closely resembles those of *A. juikitam* (Figs 5C, 6C, 7C), *A. araucaria* and *A. thomei* (Almeida & Angulo, 2006; Carvalho *et al.*, 2019b). The calls of the four species cannot be distinguished from each other in any of the call traits analysed (Table 3). Both Atlantic Forest species (*A. araucaria* and *A. thomei*) are distantly related and allopatric in relation to the Amazonian *A. kayapo* (Supporting Information, Fig. S1). In contrast, *A. juikitam* and *A. kayapo* have sympatric populations in the Cerrado-Amazonia ecotone (Figs 1B, 2B), but they occupy distinct habitats (preferentially open formations and forests, respectively). Even so, *A. kayapo* differs from the other three species by the presence of antebrachial tubercles (see morphological comparisons in the previous paragraph).

Description of holotype (Fig. 11A–B): Body robust. Snout subovoid in dorsal view, acuminate in lateral view. Nostril closer to the snout tip than to the eye; fleshy ridge on snout tip; canthus rostralis not marked; loreal region slightly concave; supratympanic fold from the posterior corner of the eye to the base of the arm; postcommissural gland ovoid; vocal sac subgular with a fold from jaw extending to forearm, vocal slit present; vomerine teeth in two straight rows medial and posterior to choanae and oblique to sagittal plane. Tongue elongated, free from the posterior half. Relative finger lengths IV < I ≃ II < III; fingers without ridges or fringes; finger tips rounded, unexpanded; inner metacarpal tubercle ovoid; outer metacarpal tubercle rounded. Subarticular tubercles nearly rounded; supernumerary tubercles rounded. Antebrachial tubercles on underside of forearm rounded. Anterior dorsum and forelimbs smooth; posterior dorsum and flank warty; tubercles on posterior dorsum, dorsal surface of hindlimb, and posterior surface of tarsus. Dorsolateral fold absent. Paracloacal gland poorly defined. Ventral surface of body and limbs mostly smooth; underside of thigh granular. Relative toe lengths I < II < V < III < IV; lateral fringing and webbing absent; tips of toes II–III slightly expanded (character states B–C), tip of toe I unexpanded, tips of toes IV–V desiccated. Inner metatarsal tubercle nearly rounded, outer metatarsal tubercle ovoid, inner tubercle twice in maximum diameter than outer tubercle. Tarsal fold extending 2/3 of tarsus length, from the inner metatarsal tubercle towards the heel. Subarticular and supernumerary tubercles nearly rounded or subconical. Measurements (in mm): SVL 17.6, HL 5.6, HW 6.6, ED 1.6, TD 1.3, EN 1.1, IND 1.5, HAL 3.7, TL 7.7, THL 7.3, FL 6.9.

Snout tip with a faded white coloration (coincident with the fleshy ridge). Dots and flecks on the upper lip off-white. Postcommissural gland off-white medially and surrounded by dark brown coloration. Tympanum light brown. Dorsal surfaces mostly dark brown intermingled with lighter shades of brown. Flecks on dorsal surface of forelimb and foot off-white, hand partially off-white. Mid-dorsal longitudinal stripe and dorsolateral stripe absent. Flank mottled. Posterior surface of thigh finely mottled in shades of brown and yellow. Ventral surface of belly and thigh partially translucent, light cream. Blotches on lower jaw off-white. Throat and anterior chest finely dark-mottled, especially following the lateral expansion of the vocal sac. Belly brown-dotted, more densely coloured laterally. Underside of forearm dark brown. Ventral surface of hand, foot and digits brown, subarticular and supernumerary tubercles and tips of fingers and toes cream-coloured. Thigh brown-dotted.

Colour of holotype in life (Fig. 9A–B): Dorsum nearly solid dark brown intermingled with lighter shades of brown. Base of arm, postcommissural gland and glands on dorsum and flank in varying shades of orange. Snout tip with a faded white coloration. Flecks on upper and lower lips light grey, extending posteriorly to the base of arm. Mid-dorsal longitudinal stripe absent, even though there is an indication as a row of orange-coloured spots arranged longitudinally. Iris deep copper. Tympanum greyish brown. Ventral surfaces mottled dark brown and off-white varying in colour prevalence. Throat finely brown-mottled; belly sparsely brown-dotted medially on a white and cream background, white and brown mottled laterally. Groin with yellow tints. Ventral surface of forelimb and hindlimb partially translucent, violet.

Variation in type specimens: Snout shape in dorsal view subovoid tending to subelliptical (MPEG

41692) or rounded (MPEG 41619). In the female (MPEG 41620), nearly rounded from above, rounded in profile; snout tip lacks a fleshy ridge or a faded white coloration; postcommissural gland nearly rounded and canthus rostralis rounded; more evident than in male specimens. MPEG 41620 and 41694 have a single, rounded antebrachial tubercle on underside (distal edge) of forearm (at least two tubercles in other specimens). In life, ventral coloration of specimens from São Félix do Xingu (photographs not directly associated with preserved specimens) vary from white-and-grey mottled to bright yellow, especially in one female. In preserved specimens, dorsolateral stripe and mid-dorsal longitudinal stripe, pale brown or grey, in CFBH 43886, MPEG 41620 and MPEG 41692. Indication of mid-dorsal longitudinal stripe in AAG-UFU 6245–6246 and MPEG 41619. Paratypes have the dorsal surface of limbs dark brown cross-banded on a lighter brown background colour. Paracloacal gland absent in MPEG 41620 and 41694, well developed in MPEG 41619, yellowish cream bordered by dark coloration of posterior surface of thigh. AAG-UFU 6245 and MPEG 41619 have lighter belly coloration, with brown dots sparsely distributed, rather than the speckled pattern (densely distributed laterally).

Advertisement call: Description based on calls of four males (N = 50 notes and 712 pulses quantified; Table 3). The call (Figs 5D, 6D, 7D) consists of a single-note, pulsed signal given at a low rate of 23–33 (28 ± 4; N = 4) notes per minute. Notes are formed by 12–16 (14 ± 1.0) partly fused pulses given at a rate of 89–131 (108 ± 16) per second and varying in duration from 3–25 (10 ± 1) ms. Note duration varies from 116–156 (139 ± 15) ms and note rise time from 37–74 (54 ± 8)% of note duration. The note frequencies are harmonically structured and the dominant frequency may coincide either with the fundamental harmonic (2304 Hz; N = 1 male) or the second harmonic (4570–4992, 4789 ± 137 Hz; N = 3 males). Frequency modulation, when present, is upward, ranging from 0–938 (553 ± 162) Hz.

Habitat and natural history: A. kayapo is usually associated with non-flooded forest habitats (*terra firme* forests) in eastern Brazilian Amazonia, although calling males have also been heard at the egde of forest clearings. Males call exposed or under the leaf litter and have calling activity concentrated during the daytime, especially in late afternoon. *A. kayapo* is sympatric with two other species of *Adenomera* at its type locality: *A. phonotriccus* is partly syntopic with *A. kayapo* at the type locality (Palestina do Pará), although they have been heard, in almost all cases, in two distinct forest fragments split by a strip of pasture land; *A. hylaedactyla*, different from *A. kayapo* and *A. phonotriccus*, occupies open areas (e.g. pastures and open vegetational types alongside with dirt roads). *A. andreae* has never been sampled at the type locality of *A. kayapo*, but they are syntopic species at Serra do Jaguar (São Félix do Xingu).

Distribution: The occurrence of *A. kayapo* is associated with the Xingu-Tocantins interfluve, comprising the type locality and some other localities on the west bank of the middle-lower Araguaia River in eastern Pará and north-eastern Mato Grosso, and single localities on the opposite bank of the river in northern Tocantins and on the east bank of the lower Xingu River (Fig. 2B). Given that the closely related *A. kayapo* and *A. phonotriccus* are morphologically cryptic species, we based their distribution ranges on acoustic and molecular data; *A. kayapo* is more widely distributed in the interfluvial region, whereas *A. phonotriccus* is restricted to two nearby localities on the west bank of the lower Araguaia River in eastern Pará (Carvalho *et al.*, 2019c).

Remarks: We had access to calls of one individual from Altamira (FNJV 11208) that are similar to the call of *A. kayapo*. However, there is a issue related to the municipal limits of Altamira, which encompass both margins of the Xingu River. Due to the lack of a specific location or coordinates, it is impossible to ascertain whether *A. kayapo* was recorded within the Xingu-Tocantins interfluve or on its opposite margin, on the west bank of the Xingu River. A field expedition to the lower Xingu River should focus on a systematic sampling on both west and east banks of the river in order to confirm the westernmost distribution range of *A. kayapo* and the potential occurrence of other species of the *A. heyeri* clade.

ADENOMERA AMICORUM, SP. NOV.

SANTARÉM TERRESTRIAL NEST-BUILDING FROG

(FIGS 2B, 3–4, 5E, 6E, 7E, 9C–D, 11C–D; TABLES 1-3)

lsid urn:lsid:zoobank.org:act:EF6EBAF5-D891-4729-B832-B3F3994BDB05

Holotype: INPA-H 40506 (field #APL 122325), adult male, BRAZIL, Pará, Belterra, Fazenda Treviso, 3.149111°S, 54.840278°W, 104 m, 12-ii-2007, A.P. Lima (Collector).

Paratypes: CFBH 44465–44469 (field #APL 122328–31, 122333, respectively), INPA-H 40490–40499,

40501–40505, 40507–40508 (field #19A–22A, APL 122305, 122311, 122313–16, 122319–21, 122323–24, 122326–27, respectively), adult males, and INPA-H 40500 (field #APL 122317), adult female, collected at the type locality between 2004–2007, A.P. Lima (Collector). INPA-H 40509–40510 (field #APL 22086, 22171, respectively), adult males, BRAZIL, Pará, Belterra, Área de Preservação Ambiental (APA) Alter do Chão, 3.516944°S, 55.073056°W, 155 m, 19-iii-2017, A.P. Lima (Collector).

Referred specimens: The genetic voucher MTR 11092: BRAZIL, Pará, Belterra, FLONA do Tapajós.

Etymology: The epithet is derived from Latin *amica*, friend, as a plural noun in apposition. The name is a reference to the members of the '*Allobates femoralis* project' led by one of us (A.P.L.) throughout Brazilian Amazonia. The research team was out in the field at the type locality of the species when it was first discovered in the early 2000s.

Diagnosis: A. amicorum is characterized by the following combination of character states: (1) medium size (adult male SVL = 20.9–24.0 mm); (2) robust body shape; (3) toe tips moderately to fully expanded (character states C–D); (4) distal antebrachial tubercle on underside of forearm; (5) two possible chromotypes (presence/absence) of dorsolateral stripe; (6) multi-note advertisement call; (7) call notes formed by 4–10 partly fused pulses; (8) note duration varying from 133–197 ms; (9) note dominant frequency coinciding with the second harmonic (3898–4221 Hz); and (10) note fundamental frequency ranging from 1958–2110 Hz.

Comparisons with congeners: A. amicorum has adult males (SVL = 20.9–24.0 mm; Table 2) smaller than those of *A. lutzi* [25.7–33.5 mm (Kok *et al.*, 2007)] and *A. simonstuarti* [25.9–26.2 mm (Angulo & Icochea, 2010)]. *A. amicorum* has a robust body shape (Fig. 11C–D), whereas *A. diptyx*, *A. martinezi* and *A. saci* have a slender body (Carvalho & Giaretta, 2013b). *A. amicorum* has toe tips moderately (character state C) or fully expanded into small discs (character state D), whereas the toe tips are unexpanded (character states A–B) in *A. bokermanni*, *A. coca*, *A. diptyx*, *A. hylaedactyla*, *A. martinezi*, *A. saci* and *A. thomei*. *A. amicorum* is distinguished from most congeners (except *A. cotuba*, *A. kayapo*, *A. lutzi* and *A. phonotriccus*) by having an antebrachial tubercle on underside of forearm. *A. amicorum* is distinguished from *A. cotuba*, which does not have a dorsolateral stripe, by the occurrence of two possible chromotypes (presence/absence) of the stripe. *A. amicorum* can be distinguished from the closely related *A. kayapo* and *A. phonotriccus* by having toe tips moderately to fully expanded (unexpanded or slightly expanded in the other two species). However, these three species are more easily distinguished from each other based on their calls. The advertisement call of *A. amicorum* (Figs 5E, 6E, 7E; Table 3) is given as multi-note calls. Such a call pattern distinguishes the new species from congeners having single-note calls, either pulsed or non-pulsed (Table 3). The other two species of *Adenomera* with multi-note calls are *A. cotuba* (Fig. 5B) and *A. simonstuarti* (T.R. de Carvalho, pers. obs.), from which the new species is distinguished by having call notes with higher frequencies in the first two harmonics and with longer duration, respectively (Table 3).

Description of holotype (Fig. 11C–D): Body robust. Snout subovoid to rounded in dorsal view, acuminate in lateral view. Nostril closer to the snout tip than to the eye; fleshy ridge on snout tip; canthus rostralis rounded; loreal region slightly concave; supratympanic fold from the posterior corner of the eye to the base of the arm; postcommissural gland elongated; vocal sac subgular with a fold from jaw extending to forearm, vocal slit present; vomerine teeth in two straight rows medial and posterior to choanae and oblique to sagittal plane. Tongue elongated, free from the posterior half. Relative finger lengths IV ≃ I < II < III; fingers without ridges or fringes; finger tips rounded, slightly expanded; inner metacarpal tubercle ovoid; outer metacarpal tubercle nearly rounded. Subarticular tubercles rounded or nearly rounded; supernumerary tubercles rounded. Antebrachial tubercle on underside of forearm, single, rounded. Anterior dorsum and forelimb smooth; posterior dorsum and flank warty; tubercles sparsely distributed on posterior dorsum, dorsal surface of hindlimb and posterior surface of tarsus. Dorsolateral fold absent. Paracloacal gland indistinct; lumbar gland rounded. Ventral surface of body and limb mostly smooth; underside of thigh granular. Relative toe lengths I < II < V < III < IV; lateral fringing and webbing absent; tips of toes II–IV moderately expanded (character state C), tips of toes I and V unexpanded. Inner metatarsal tubercle ovoid, outer metatarsal tubercle nearly rounded, inner tubercle twice the maximum diameter of the outer tubercle. Tarsal fold extending 1/2 of tarsus length, from the inner metatarsal tubercle towards the heel, with a short gap close to the tubercle. Subarticular tubercles nearly rounded or subconical; supernumerary tubercles nearly rounded. Measurements (in mm): SVL 21.7, HL 6.8, HW 8.1, ED 1.9, TD 1.3, EN 1.6, IND 1.9, HAL 4.4, TL 9.5, THL 8.9, FL 10.0.

Snout tip with a faded white coloration (coincident with the fleshy ridge). Blotches on the upper lip faded white. Postcommissural gland cream-coloured. Tympanum light brown. Dorsum and dorsal surface of hindlimb brown on a light brown background. Flank speckled in light brown on a light grey background.

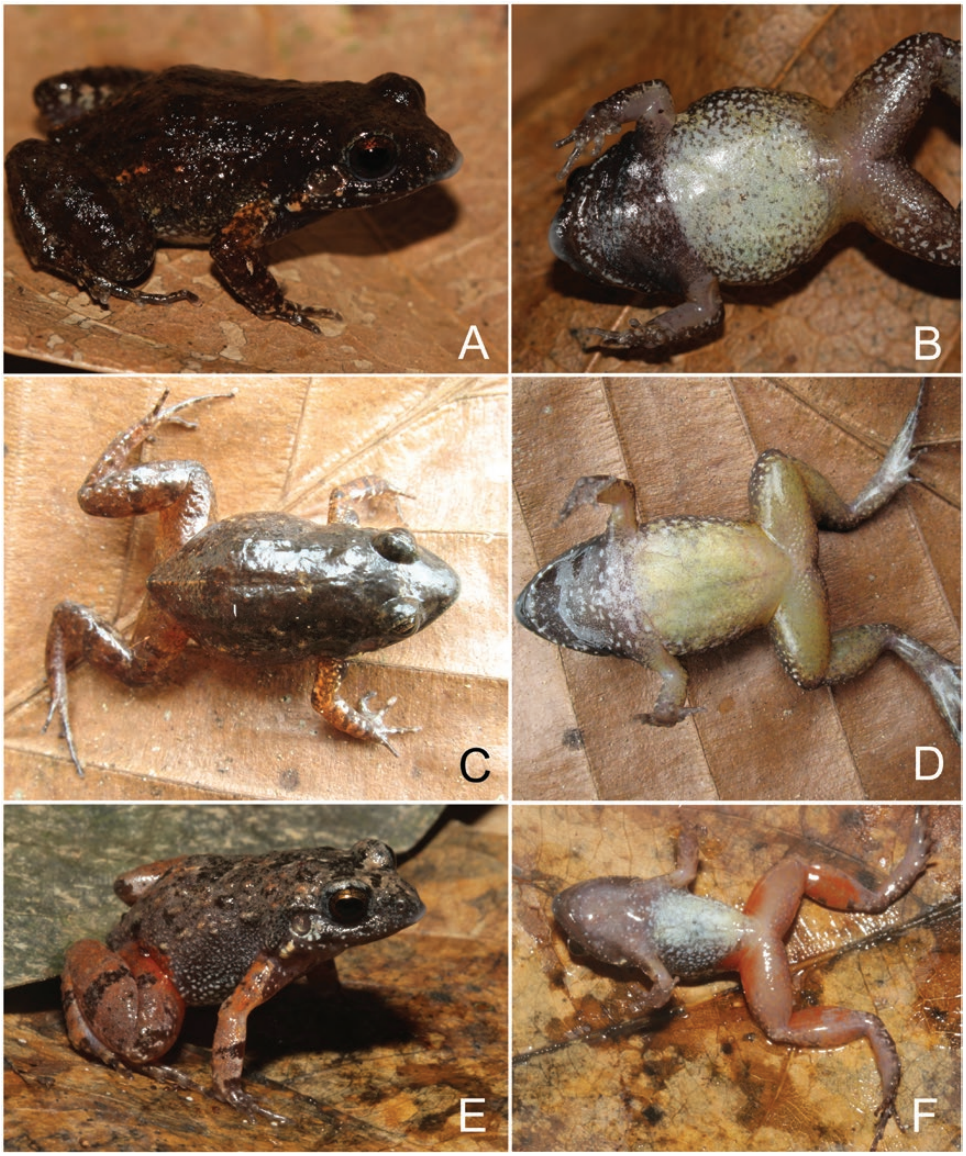

Figure 9. Life colours (adult males) of three new species of the *A. heyeri* clade from their type localities in Brazilian Amazonia. A–B, holotype of ***A. kayapo*** (CFBH 43885: SVL = 17.6 mm). C–D, paratype of ***A. amicorum*** (INPA-H 40497: SVL = 22.7 mm). E–F, holotype of ***A. aurantiaca*** (INPA-H 40520: SVL = 20.9 mm). Photographs of *A. aurantiaca* by José Cassimiro.

Posterior surface of thigh finely mottled in shades of brown and yellow. Mid-dorsal longitudinal stripe and dorsolateral stripes absent. Paracloacal gland pale yellow, covered with melanophores. Ventral surface of belly and thigh partially translucent, yellowish cream. Blotches on lower jaw white. Throat and anterior chest brown-dotted and white-spotted. Fine mottling (brown) faded. Underside of forearm brown. Ventral surface of hand, foot and digits have brown, subarticular and supernumerary tubercles, and tips of fingers and toes are cream-coloured and light grey. Brown spotting sparsely distributed on thigh.

Variation in type specimens: Overall coloration is faded in the specimens INPA-H 40490–93. Their throat varies in brown mottling intensity. INPA-H 40494 has snout subovoid to subelliptical in dorsal view; throat coloration faded; paracloacal gland absent. The female INPA-H 40500 has snout nearly rounded from above, rounded in profile; dorsolateral fold pale yellow, indication of mid-dorsal longitudinal stripe, paracloacal gland absent; hindlimbs mostly smooth. Dorsolateral folds and/or stripes are present in INPA-H 40497, 40500, 40502–04, 40507, 40509. Tips of toes II–IV vary between moderately to fully expanded (character

states C–D) in CFBH 44468–69, INPA-H 40490–98, 40500 and 40502, and are fully expanded (state D) in INPA-H 40499, 40501 and 40505. Paracloacal and lumbar glands, and antebrachial tubercles may be low or flattened, and have the same colour of background dorsal/ventral coloration, which make them difficult to observe even under magnification. The holotype was not photographed in life; however, life colours of a paratype are shown in Fig. 9C–D.

Advertisement call: Description based on calls of three males (N = 134 notes and 980 pulses quantified; Table 3). The call (Figs 5E, 6E, 7E) consists of a multi-note signal given a few times (2–7) per minute. Calls are composed of 3–9 (5 ± 2; N = 3) notes given at a rate of 1–2 (2 ± 1; N = 3) per second. Notes are formed by 4–10 (7 ± 1) partly fused pulses given at a rate of 43–67 (51 ± 4) per second and varying in duration from 3–62 (22 ± 1) ms. Note duration varies from 133–197 (162 ± 6) ms and note rise time from 38–74 (55 ± 4)% of note duration. The note frequencies are harmonically structured and the dominant frequency coincides with the second harmonic (3898–4221, 4047 ± 38 Hz). The note fundamental frequency ranges from 1958–2110 (2029 ± 42) Hz. Frequency modulation is upward in most cases, with a few calls modulating slightly downward, varying from –129 to 1206 (330 ± 367) Hz.

Habitat and natural history: Several males of *A. amicorum* were heard calling hidden under the leaf litter in an old-growth non-flooded forest during daytime throughout most of rainy season (November to March). *A. andreae* and *A. hylaedactyla* are sympatric with the new species at the type locality.

Distribution: A. amicorum is known from the type locality and FLONA Tapajós, both within the municipal limits of Belterra (Fig. 2B). The species was also acoustically registered from other localities on the east bank of the lower Tapajós River (Rurópolis, Placas and Uruará); however, recordings and tissue samples are not available for the confirmation of these occurrence points for the species.

Remarks: There is a single specimen from the west bank of the Xingu River associated with the lineage sp. F2 (=*A. amicorum*), the genetic voucher BM 23 from UHE Belo Monte, in Vitória do Xingu (Supporting Information, Appendix S2). The genetic divergence between this specimen and type specimens of *A. amicorum* matches exactly the 5% threshold of interspecific divergence in our species delimitation analysis (Table 1). Further information, especially sound recordings, will be required for an accurate assessment of the taxonomic identity of the Xingu population. For the moment, the voucher BM 23 is pending a definite species assignment, referred herein to as *A.* cf. *amicorum*.

ADENOMERA AURANTIACA, SP. NOV.

ORANGE-LEGGED TERRESTRIAL NEST-BUILDING FROG

(FIGS 2B, 3–4, 5G, 6G, 7G, 9E–F, 11E–F; TABLES 1-3)

lsid urn:lsid:zoobank.org:act:EA632E5E-083B-4DAC-AA8A-67C513AFDD20

Holotype: INPA-H 40520 (field #DT 4327), adult male, BRAZIL, Pará, Trairão, 4.756617°S, 56.394333°W, 91 m, 30-x-2013, D. Pavan (Collector).

Paratypes: INPA-H 40518 (field #DT 3486), adult female, INPA-H 40519 (field #DT 4272), subadult, and INPA-H 40521 (field #DT 4117), juvenile, BRAZIL, Pará, Trairão, 4.883550–5.073200°S, 56.437950–56.440050°W, 78–102 m, between 2012–2013, D. Pavan and L.J.C.L. Moraes (Collectors).

Etymology: The epithet is derived from the Latin *aurantiacus*, the colour orange, referring to the brightly orange-coloured limbs of this species. Such a colour appears to be unique in the genus *Adenomera*.

Diagnosis: A. aurantiaca is characterized by the following combination of character states: (1) medium size (both adult specimens, one male and one female, with SVL = 20.9 mm); (2) robust body shape; (3) toe tips slightly to moderately expanded (character states B–C); (4) distal antebrachial tubercle on underside of forearm; (5) belly white and grey mottled, especially in life; (6) thigh surfaces brightly orange-coloured, especially in life; (7) multi-note advertisement call; (8) call notes formed by 5–7 complete pulses; (9) note duration varying from 112–137 ms; (10) note dominant frequency coinciding with the second harmonic (4102–4523 Hz); and (11) note fundamental frequency ranging from 2074–2246 Hz.

Comparisons with congeners: A. aurantiaca has adult specimens (SVL = 20.9 mm; Table 2) smaller than those of *A. coca* [23.6–25.6 mm (Angulo & Reichle, 2008)], *A. lutzi* [25.7–33.5 mm (Kok *et al.*, 2007)] and *A. simonstuarti* [25.9–26.2 mm (Angulo & Icochea, 2010)]. *A. aurantiaca* has a robust body shape (Fig. 11E–F), whereas *A. diptyx*, *A. martinezi* and *A. saci* have a slender body. *A. aurantiaca* has slightly to moderately expanded toe tips (character states B–C), but not fully expanded into small discs (character state D) as in *A. ajurauna*, *A. andreae*, *A. chicomendesi*, *A. heyeri*, *A. marmorata*, *A. lutzi*, *A. nana* and *A. simonstuarti*. *A. aurantiaca* is distinguished from congeners (except *A. amicorum*,

A. cotuba, *A. kayapo*, *A. lutzi* and *A. phonotriccus*) by having an antebrachial tubercle on underside of forearm. *A. aurantiaca* differs from *A. araucaria*, *A. bokermanni*, *A. heyeri*, *A. kweti*, *A. lutzi* and *A. nana* by having ventral surfaces mottled white and grey (Fig. 9F)—these are yellow or sometimes with yellowish tints in the other species. *A. aurantiaca* is further distinguished from congeners by having orange-coloured limbs, particularly bright orange on the thigh and groin in life (Figs 9E–F). Other *Adenomera* species might have tints of orange and yellow on groin and hindlimbs; however, *A. aurantiaca* is the only species in the genus exhibiting a bright orange colouration, extending also over the shank and tarsus. The advertisement call of *A. aurantiaca* (Figs 5G, 6G, 7G; Table 3) is given as multi-note calls. Such a call pattern distinguishes the new species from congeners having single-note calls, either pulsed or non-pulsed (Table 3). The only three species of *Adenomera* with multi-note calls are *A. amicorum* (Fig. 5E), *A. cotuba* (Fig. 5B) and *A. simonstuarti* (T.R. de Carvalho, pers. obs.), from which the new species is distinguished by having notes with complete pulses (call notes with partly fused pulses in the other three species).

Description of holotype (Fig. 11E–F): Body robust. Snout rounded in dorsal view, acuminate in lateral view. Nostril closer to the snout tip than to the eye; fleshy ridge on snout tip; canthus rostralis rounded; loreal region slightly concave; supratympanic fold from the posterior corner of the eye to the base of the arm; postcommissural gland ovoid; vocal sac subgular with a fold from jaw extending to forearm, vocal slit present; vomerine teeth in two straight rows medial and posterior to choanae and oblique to sagittal plane. Tongue elongated, free from the posterior third. Relative finger lengths IV < I ≃ II < III; fingers without ridges or fringes; finger tips rounded, slightly expanded in fingers I and IV; inner metacarpal tubercle ovoid; outer metacarpal tubercle nearly rounded. Subarticular tubercles nearly rounded; supernumerary tubercles rounded. Antebrachial tubercle on underside of forearm, single, nearly rounded. Dorsum mostly smooth, flank warty. Tubercles on posterior surface of tarsus. Ventral surface of body smooth; underside of thigh granular. Paracloacal gland nearly rounded. Relative toe lengths I < II < V < III < IV; lateral fringing and webbing absent; tips of toes II–IV moderately expanded (character state C), tip of toe I unexpanded, tip of toe V slightly expanded. Inner metatarsal tubercle ovoid, outer metatarsal tubercle nearly rounded, inner tubercle twice the maximum diameter of the outer tubercle. Tarsal fold extending 1/2 of tarsus length, from the inner metatarsal tubercle ending in a tubercle separated from the fold by a short gap. Subarticular tubercles nearly rounded or subconical; supernumerary tubercles rounded. Measurements are given in Table 2.

Snout tip with a faded white coloration (coincident with the fleshy ridge). Blotches on the upper lip white. Postcommissural gland mostly covered with melanophores light grey and dark brown. Tympanum light brown. Dorsal surface of body and limbs varying from light to dark brown; forelimbs brown and cream-coloured. Body with darker, large blotches and off-white smaller blotches in the last third of body length; limbs with dark brown transverse bars. Posterior surface of thigh pale yellow with scattered brown stains; paracloacal gland off-white. Dorsolateral stripe absent; an indication of a mid-dorsal longitudinal line, fragmented and mostly indistinct, light brown. Throat, chest, belly and underside of limbs partly translucent, cream-coloured. Spots on throat and chest white on a fine brown mottling; belly brown-mottled. Underside of forearm (outer margin), palm of hand, sole of foot, digits and subarticular tubercles mostly brown and light grey; tips of fingers and toes non-pigmented.

Colour of holotype in life (Fig. 9E–F): Dorsum covered with black speckles and spots irregularly distributed on a grey and brown background. Iris copper. Tympanum dark brown. Dorsal surface of arms, legs and groin bright orange and brown. Mid-dorsal longitudinal stripe light grey, postcommissural gland yellow, white and dark grey. Flank white and dark grey mottled. Throat and chest with white speckles on a dark brown background, belly white and grey, intensely mottled laterally. Ventral surface of legs bright orange, violet and light grey.

Variation in type specimens: Variation is restricted to colour patterns, which are related to mottling on belly (extensive or sparse) and throat (colour intensity, spotted/mottled). The female INPA-H 40518 has the snout shape nearly rounded from above and rounded in profile, fleshy ridge and paracloacal gland absent.

Advertisement call: Description based on calls of two males (N = 23 notes and 135 pulses quantified; Table 3). The call (Figs 5G, 6G, 7G) consists of a multi-note signal given once or twice per minute. Calls are composed of 8–12 (9 ± 2; N = 2) notes given at a rate of 2–3 (2 ± 1; N = 2) per second. Notes are formed by 5–7 (6 ± 1) complete pulses given at a rate of 40–69 (51 ± 3) per second and varying in duration from 5–36 (13 ± 1) ms. Note duration varies from 112–137 (122 ± 4) ms and note rise time from 38–78 (50 ± 8)% of note duration. The note frequencies are harmonically structured and the dominant frequency coincides with the second harmonic (4102–4523, 4337 ± 86 Hz). The note fundamental frequency ranges from 2074–2246 (2120 ± 42) Hz. Frequency

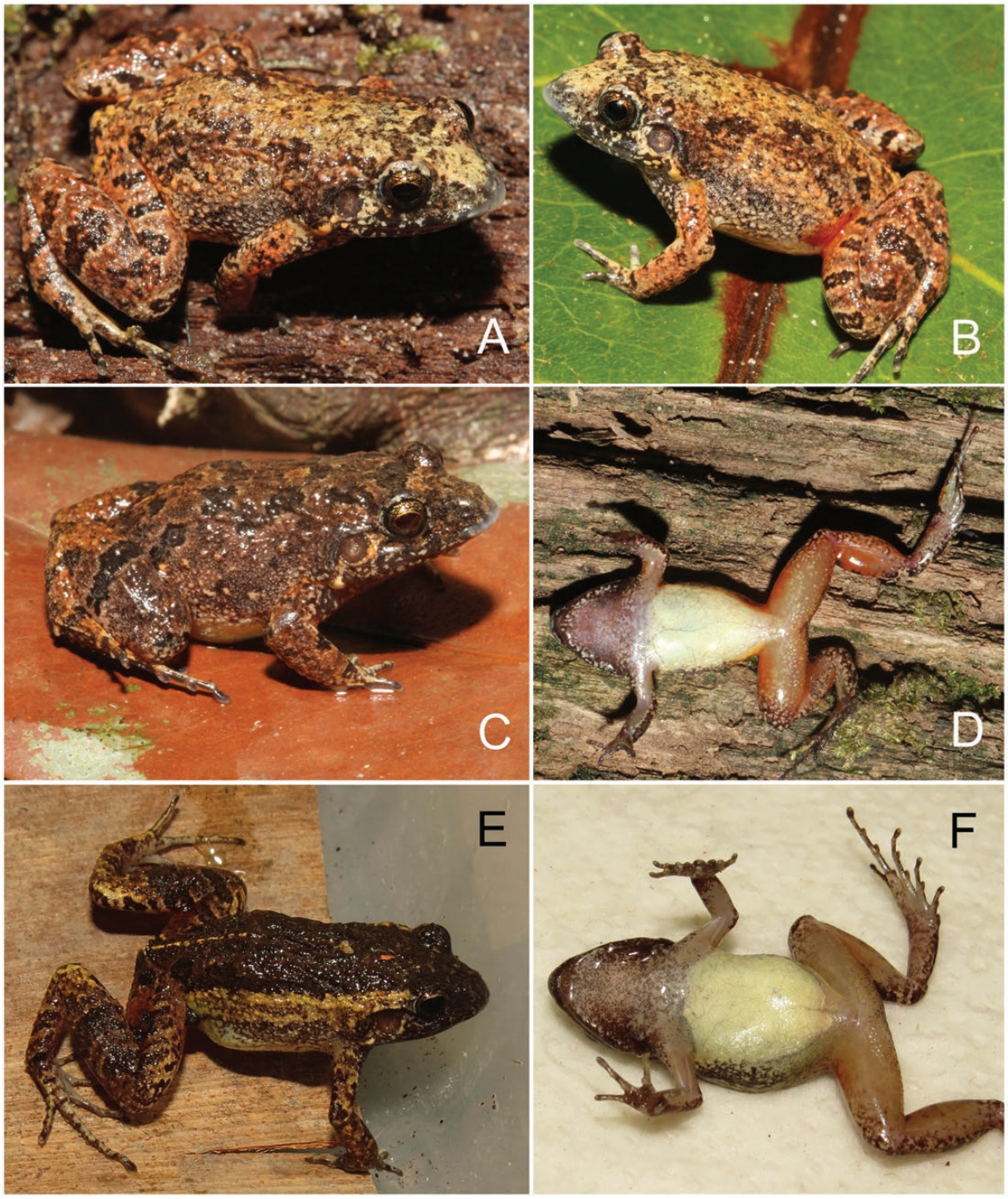

Figure 10. Life colours (adult males) of three new species of the *A. heyeri* clade from their type localities in Brazilian Amazonia. A–B, holotype of ***A. inopinata*** (INPA-H 40517: SVL = 23.5 mm). C–D, holotype of ***A. tapajonica*** (INPA-H 40516: SVL = 23.6 mm). E–F, paratype of ***A. gridipappi*** (CFBH 44470: SVL = 27.6 mm). Photographs of *A. tapajonica* by José Cassimiro.

modulation is upward in most cases, with a single call modulating slightly downward, varying from –47 to 609 (408 ± 96) Hz.

Habitat and natural history: *A. aurantiaca* inhabits non-flooded primary forests, even though the species appears to occupy clearing sites with some sunlight

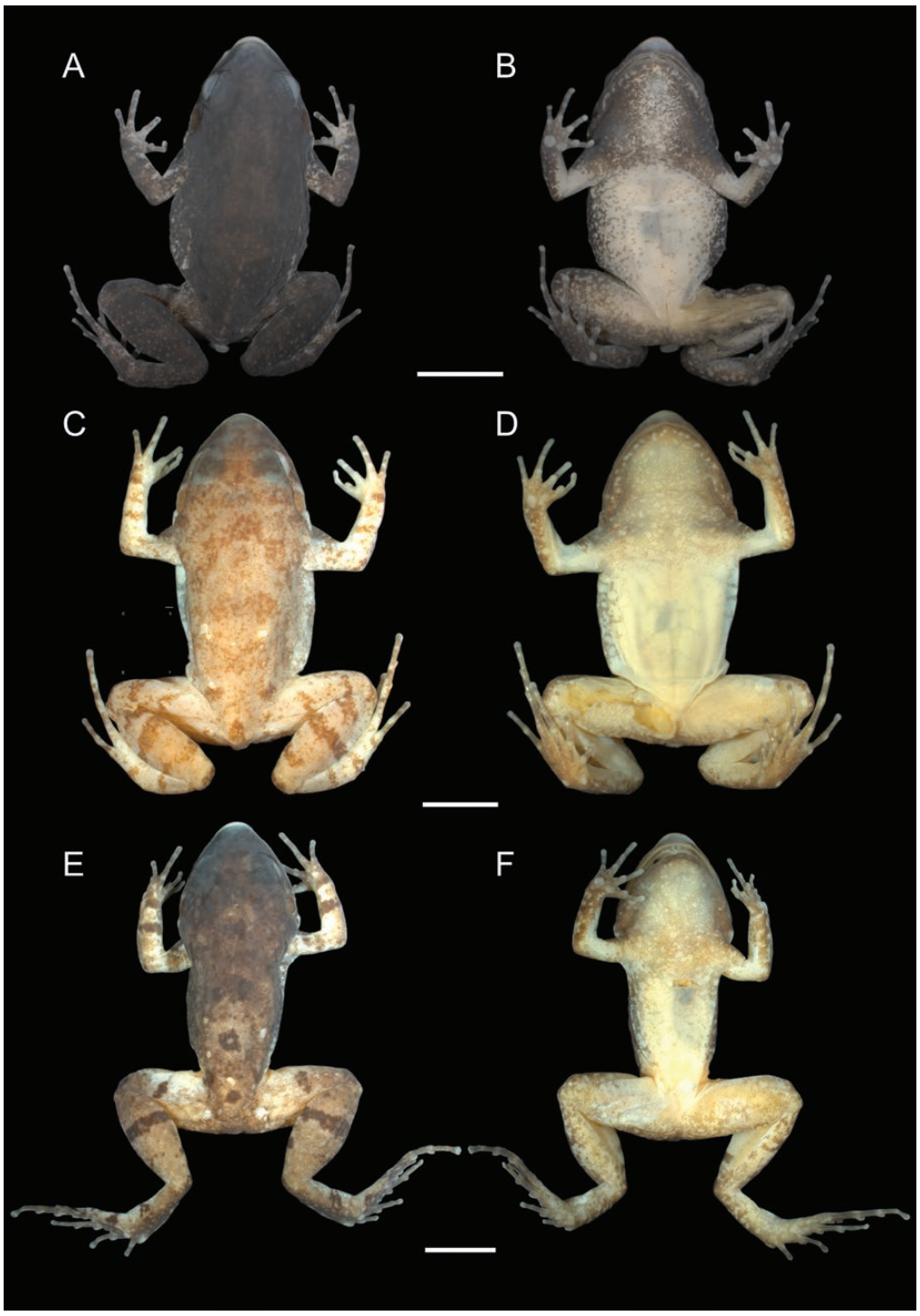

Figure 11. Dorsal and ventral body of three new species of the *A. heyeri* clade (holotypes). A–B, ***A. kayapo*** (CFBH 43885). C–D, ***A. amicorum*** (INPA-H 40506). E–F, ***A. aurantiaca*** (INPA-H 40520). Scale = 5 mm.

as a preferred calling habitat. The breeding season is concentrated at the onset of the rainy season (October–November), when several males can be heard during the daytime, calling hidden amidst clumps of fallen branches on the forest floor or next to the base of terrestrial palm trees. *A. andreae* is the only congener found syntopically with the new species.

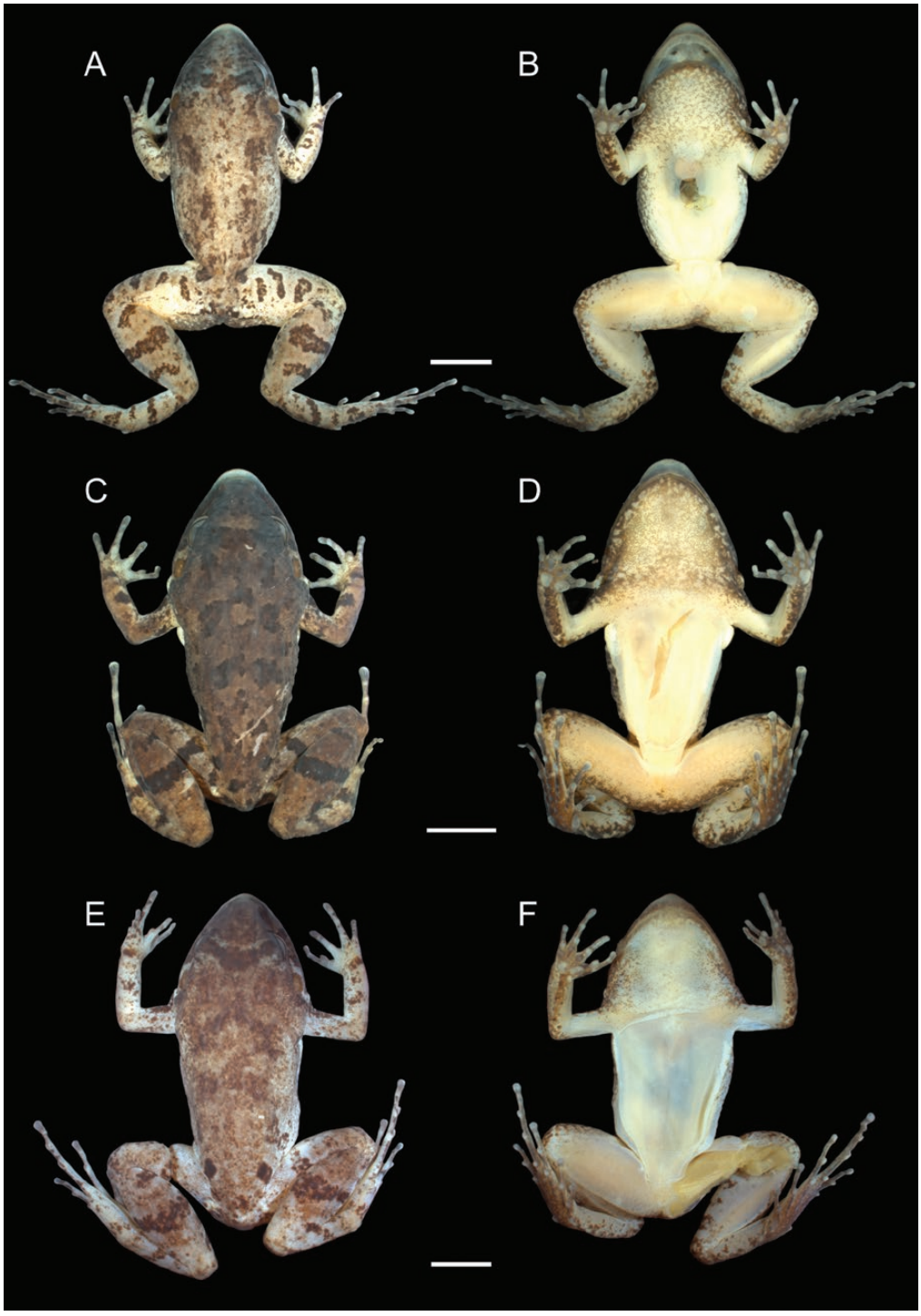

Figure 12. Dorsal and ventral body of three new species of the *A. heyeri* clade (holotypes). A–B, ***A. inopinata*** (INPA-H 40517). C–D, ***A. tapajonica*** (INPA-H 40516). E–F, ***A. gridipappi*** (INPA-H 40512). Scale = 5 mm.

Distribution: A. aurantiaca is associated with lowland forests on the east bank of the middle Tapajós River in eastern Brazilian Amazonia. The distribution range appears to be limited to the east bank of the Jamanxim River (Fig. 2B).

ADENOMERA INOPINATA, SP. NOV.

UNFORESEEN TERRESTRIAL NEST-BUILDING FROG

(FIGS 2B, 3–4, 5H, 6H, 7H, 10A–B, 12A–B; TABLES 1-3)

lsid urn:lsid:zoobank.org:act:E21553B7-A8CC-495A-8056-E8C203A7A9B6

Holotype: INPA-H 40517 (field #DT 3923), adult male, BRAZIL, Pará, Itaituba, 5.240183°S, 56.915383°W, 143 m, 13-xii-2012, J. Gomes (Collector).

Etymology: The epithet is derived from the Latin *inopinatus*, unexpected, referring to the unexpected discovery of this species in the region of the middle Tapajós River, where two other unnamed *Adenomera* species described in the present study had already been collected when *A. inopinata* was discovered (see Fig. 2).

Diagnosis: A. inopinata is characterized by the following combination of character states: (1) medium size (adult male SVL = 23.5 mm); (2) robust body shape; (3) toe tips moderately expanded (character state C); (4) distal antebrachial tubercle on underside of forearm; (5) multi-note advertisement call; (6) call notes formed by 4–5 complete pulses; (7) note duration varying from 70–91 ms; and (8) note dominant frequency coinciding with the fundamental harmonic (2109–2203 Hz).

Comparisons with congeners: A. inopinata (adult male SVL = 23.5 mm; Table 2) is smaller than *A. lutzi* [25.7–33.5 mm (Kok *et al.*, 2007)] and *A. simonstuarti* [25.9–26.2 mm (Angulo & Icochea, 2010)] and larger than *A. ajurauna* [17.2–20.0 mm (Berneck *et al.*, 2008)], *A. araucaria* [17.4–19.3 mm (Carvalho *et al.*, 2019b)], *A. aurantiaca* (20.9 mm), *A. kweti* [15.4–19.3 mm (Carvalho *et al.*, 2019b)], *A. kayapo* (17.5–21.0 mm), *A. nana* [16.3–19.4 mm (Kwet, 2007)] and *A. phonotriccus* [19.8–21.6 mm (Carvalho *et al.*, 2019c)]. *A. inopinata* has a robust body shape (Fig. 12A–B), whereas *A. diptyx*, *A. martinezi* and *A. saci* have a slender body. *A. inopinata* has moderately expanded toe tips (character state C), but not fully expanded into small discs (character state D) as in *A. ajurauna*, *A. amicorum*, *A. andreae*, *A. chicomendesi*, *A. heyeri*, *A. marmorata*, *A. lutzi*, *A. nana* and *A. simonstuarti*, or unexpanded (character states A–B) as in *A. bokermanni*, *A. coca*, *A. diptyx*, *A. hylaedactyla*, *A. martinezi*, *A. saci* and *A. thomei*. *A. inopinata* is distinguished from congeners (except *A. amicorum*, *A. aurantiaca*, *A. cotuba*, *A. kayapo*, *A. lutzi* and *A. phonotriccus*) by having an antebrachial tubercle on the underside of the forearm.

The advertisement call of *A. inopinata* (Figs 5H, 6H, 7H; Table 3) is given as multi-note calls. Such a call pattern distinguishes the new species from congeners having single-note calls, either pulsed or non-pulsed (Table 3). The other four *Adenomera* species with multi-note calls are *A. aurantiaca* (Fig. 5G), *A. cotuba* (Fig. 5B), *A. amicorum* (Fig. 5E) and *A. simonstuarti* (T.R. de Carvalho, pers. obs.), from which the new species is distinguished by having call notes with complete pulses (Figs 6H, 7H) compared to partly fused pulses in the call notes of *A. amicorum* (Figs 6E, 7E), *A. cotuba* (Figs 6B, 7B) and *A. simonstuarti* (Table 3). From the closely related *A. aurantiaca*, *A. inopinata* is mainly distinguished by having call notes with fewer pulses per note, shorter duration and the dominant frequency coinciding with the fundamental harmonic (Fig. 6G–H; Table 3). Call notes of these species also differ markedly in rise time, always coinciding with the first call note in *A. inopinata* (*A. inopinata*: 1–3% of note duration; *A. aurantiaca*: 38–78% of note duration).

Description of holotype (Fig. 12A–B): Body robust. Snout rounded in dorsal view, acuminate in lateral view. Nostril closer to the snout tip than to the eye, fleshy ridge on snout tip, canthus rostralis not marked, loreal region slightly concave, supratympanic fold from the posterior corner of the eye to the base of the arm, postcommissural gland ovoid, vocal slit present, vomerine teeth in two straight rows medial and posterior to choanae and oblique to sagittal plane. Tongue elongated, free from the posterior half. Relative finger lengths I < II ≃ IV < III, fingers without ridges or fringes, finger tips rounded, slightly expanded, especially fingers III and IV, inner metacarpal tubercle elongated, outer metacarpal tubercle rounded. Subarticular tubercles nearly rounded or rounded, supernumerary tubercles rounded. Antebrachial tubercle on underside of forearm, single, rounded. Dorsum mostly smooth, flank and inguinal region glandular. Posterior surface of thigh granular contiguous with the ventral surface. Paracloacal gland divided, nearly rounded to ovoid. Ventral surface of body and limb smooth. Relative toe lengths I < II < V < III < IV, lateral fringing and webbing absent, tips of toes II–IV moderately expanded (character state C), tips of toes I and V unexpanded. Inner and outer metatarsal tubercles ovoid, inner tubercle twice the maximum diameter of the outer tubercle. Tarsal fold low, extending 2/3 of tarsus length, from the inner metatarsal tubercle towards the heel, ending in a tubercle separated from the fold by a short gap. Subarticular tubercles nearly rounded or subconical, supernumerary tubercles rounded. Measurements are given in Table 2.

Snout tip with a faded white coloration (coincident with the fleshy ridge). Blotches on the upper lip white. Postcommissural gland cream-coloured medially and surrounded by brown coloration. Tympanum light brown. Dorsal surface of body and limbs light

brown with dark brown blotches, spots and stains. Interorbital bar dark brown. Dorsal surface of limbs with interrupted transverse bars and blotches dark brown. Posterior surface of thigh pale yellow laterally, dark brown in the cloacal region, paracloacal gland pale yellow and dark brown. Mid-dorsal longitudinal stripe and dorsolateral stripes absent. Ventral surface of belly and thigh partially translucent, yellowish cream. Throat and chest brown-mottled. Belly mostly immaculate, with brown mottling laterally. Underside of forearm (outer margin), palm of hand, sole of foot and digits brown interspersed with lighter sections in grey and cream, subarticular tubercles partly pigmented, tips of fingers and toes non-pigmented.

Colour of holotype in life (Fig. 10A–B): Dorsum covered with dark brown stains and spots irregularly distributed on a light brown background. Iris copper. Tympanum brown. Groin yellow. Postcommissural gland orange. Arms and legs with dark brown transverse stripes and stains on a reddish brown background. Information on life colours in ventral view was not assessed.

Advertisement call: Description based on calls of one male (N = 13 notes and 57 pulses quantified; Table 3). The call (Figs 5H, 6H, 7H) consists of a multi-note signal given twice per minute (based on a brief sound recording). Calls are composed of 5–10 (8 ± 4) notes given at a rate of four per second. Notes are formed by 4–5 (4 ± 1) complete pulses given at a rate of 58–63 (60 ± 1) per second and varying in duration from 5–30 (14 ± 1) ms. Note duration varies from 70–91 (79 ± 7) ms and note rise time from 1–3 (2 ± 1)% of duration. The note frequencies are harmonically structured and the dominant frequency coincides with the fundamental harmonic (2109–2203, 2189 ± 35 Hz). Frequency modulation is upward, rising 188–656 (526 ± 151) Hz.

Habitat and natural history: Due to the rarity of *A. inopinata* at the type locality, we do not have enough data to describe general aspects of the natural history and preferred calling habitat of the species. The single individual that has been recorded to date was found calling on the leaf litter of a primary non-flooded forest during the rainy season (December). The exact type locality is a location of difficult access because of the irregular terrain of rocky outcrops. It is located about 2.5 km away from the east margin of the Tapajós River. *A. andreae* is the only syntopic congener of *A. inopinata* at the type locality, much more abundant than the new species in the region.

Distribution: A. inopinata is known only from the type locality in the Tapajós-Jamanxim interfluve. *A. inopinata* occurs west of the Jamanxim River, whereas the closest related (and presumably allopatric) *A. aurantiaca* occurs on the opposite river bank (Fig. 2B).

Remarks: It is relevant to highlight the rarity of *A. inopinata* at the single location where the species is known to occur. Regardless of extensive sampling effort at the type locality of *A. inopinata* at the middle Tapajós River during two years [see detailed information in Moraes *et al.* (2016)], only a single male was ever recorded and collected.

ADENOMERA TAPAJONICA, SP. NOV.

TAPAJÓS TERRESTRIAL NEST-BUILDING FROG

(FIGS 2A, 3–4, 5I, 6I, 7I, 10C–D, 12C–D; TABLES 1-3)

lsid urn:lsid:zoobank.org:act:366E654C-AC84-42B8-9303-DC28675C9E5F

Holotype: INPA-H 40516 (field #DT 3886), adult male, BRAZIL, Pará, Itaituba, 5.052133°S, 56.876833°W, 78 m, 8-xii-2012, D. Pavan (Collector).

Paratypes: INPA-H 40515 (field #DT 3180), adult female, BRAZIL, Pará, Itaituba, 4.673833°S, 56.446717°W, 87 m, 4-vii-2012, D. Pavan (Collector). CZPB-AA 2118 (field #J153), adult male, BRAZIL, Pará, Juruti, Igarapé do Mutum, 2.611931°S, 56.185492°W, 118 m, 24-iii-2011, M. Gordo (Collector).

Etymology: The epithet is derived from the Tapajós River. The distribution range of *A. tapajonica* comprises a swathe of land entailing the west bank of the middle-lower Tapajós River, limited to the south of the Amazon River (Fig. 2A).

Diagnosis: A. tapajonica is characterized by the following combination of character states: (1) relatively large size (adult male SVL = 23.6–25.6 mm); (2) robust body shape; (3) toe tips moderately to fully expanded into small discs (character states C–D); (4) distal antebrachial tubercle on underside of forearm; (5) belly immaculate, cream-coloured; (6) thigh surfaces brightly orange-coloured, especially in life; (7) single-note advertisement call; (8) call note formed by 3–5 partly fused pulses; (9) note duration varying from 66–89 ms; and (10) note dominant frequency coinciding with the fundamental harmonic (1873–2003 Hz; N = 1 male) and second harmonic (4055–4430 Hz; N = 1 male).

Comparisons with congeners: A. tapajonica has adult males (SVL = 23.6–25.6 mm; Table 2) smaller than

those of *A. lutzi* [25.7–33.5 mm (Kok *et al.*, 2007)] and *A. simonstuarti* [25.9–26.2 mm (Angulo & Icochea, 2010)] and larger than *A. ajurauna* [17.2–20.0 mm (Berneck *et al.*, 2008)], *A. araucaria* [17.4–19.3 mm (Carvalho *et al.*, 2019b)], *A. aurantiaca* (20.9 mm), *A. kweti* [15.4–19.3 mm (Carvalho *et al.*, 2019b)], *A. kayapo* (17.5–21.0 mm), *A. nana* [16.3–19.4 mm (Kwet, 2007)] and *A. phonotriccus* [19.8–21.6 mm (Carvalho *et al.*, 2019c)]. *A. tapajonica* has a robust body shape (Fig. 12C–D), whereas *A. diptyx*, *A. martinezi* and *A. saci* have a slender body. *A. tapajonica* has toe tips that are moderately to fully expanded into small discs (character states C–D), differing from species having unexpanded or slightly expanded toe tips (character states A–B) as in *A. bokermanni*, *A. coca*, *A. cotuba*, *A. diptyx*, *A. hylaedactyla*, *A. juikitam*, *A. martinezi*, *A. saci* and *A. thomei*. *A. tapajonica* is distinguished from congeners (except *A. amicorum*, *A. aurantiaca*, *A. cotuba*, *A. inopinata*, *A. kayapo*, *A. lutzi* and *A. phonotriccus*) by having an antebrachial tubercle on underside of forearm. *A. tapajonica* differs from *A. araucaria*, *A. bokermanni*, *A. heyeri*, *A. kweti*, *A. lutzi* and *A. nana* by having belly cream-coloured (Fig. 10D), this is yellow or sometimes has yellowish tints in the other species. *A. tapajonica* can be further distinguished from some members of the *A. heyeri* clade (*A. amicorum A. kayapo* and *A. phonotriccus*) by lacking a dorsolateral stripe; such a colour feature is present in some specimens of the other three species. *A. tapajonica* is also distinguished from congeners (except *A. aurantiaca* and *A. inopinata*; Figs 9E–F, 10B) by having thighs and groin orange-coloured (Fig. 10D). From *A. aurantiaca*, *A. tapajonica* differs in thigh colour patterns in life: both species share the orange coloration; however, the major pattern in *A. aurantiaca* is brighter and more extensively distributed over the groin, hindlimbs and forelimbs (Fig. 9E–F), whereas the pattern in *A. tapajonica* is relatively duller, orange-brown, and does not extend over the dorsal surface of hindlimbs and forelimbs (Fig. 10C–D). The three new *Adenomera* species with distinctively orange-coloured thighs (*A. aurantiaca*, *A. inopinata* and *A. tapajonica*) can be distinguished from each other by their distinct calls.

The advertisement call of *A. tapajonica* (Figs 5I, 6I, 7I; Table 3) is given as single notes. Such a call pattern distinguishes the new species from congeners having multi-note calls (*A. amicorum*, *A. aurantiaca*, *A. cotuba*, *A. inopinata* and *A. simonstuarti*; Fig. 5; Table 3). *A. tapajonica* is distinguished from eight congeners with non-pulsed calls by having a pulsed call (see Table 3). From the ten congeners also having single-note, pulsed calls, *A. tapajonica* is distinguished from *A. andreae* by having a call note with a lower fundamental frequency (Table 3), from *A. coca*, *A. juikitam*, *A. martinezi* and *A. thomei* by having fewer pulses per note (Table 3), from *A. araucaria* and *A. heyeri* by a shorter note duration (Table 3), and from *A. diptyx* and *A. hylaedactyla* [combined repetition rate of 107–242 notes/min (Márquez *et al.*, 1995; Carvalho *et al.*, 2019d)] by a lower note repetition rate (87–98 ms). The call of *A. tapajonica* is formed by partly fused pulses (Figs 6I, 7I), whereas that of *A. phonotriccus* is formed by complete pulses (Figs 6F, 7F).

Description of holotype (Fig. 12C–D): Body robust. Snout subovoid to rounded in dorsal view, acuminate in lateral view. Nostril closer to the snout tip than to the eye, fleshy ridge on snout tip, canthus rostralis not marked, loreal region slightly concave, supratympanic fold from the posterior corner of the eye to the base of the arm, postcommissural gland ovoid, vocal sac subgular with a fold from jaw extending to forearm, vocal slit present, vomerine teeth in two straight rows medial and posterior to choanae and oblique to sagittal plane. Tongue elongated, free from the posterior half. Relative finger lengths IV < I ≃ II < III, fingers without ridges or fringes, finger tips rounded, unexpanded, inner metacarpal tubercle ovoid, outer metacarpal tubercle nearly rounded. Subarticular tubercles nearly rounded, supernumerary tubercles rounded. Antebrachial tubercle single, rounded. Anterior dorsum smooth, posterior dorsum glandular, flank warty. Dorsolateral fold extending posteriorly from scapular region to the groin, dorsal fold lies behind the upper eyelid and extends posteriorly until 2/3 body length. Dorsal surface of shank and posterior surface of tarsus covered with white-tipped tubercles. Paracloacal gland indistinct. Ventral surface of body and limb mostly smooth, underside of thigh areolate/granular in contact with ventral surface. Relative toe lengths I < II < V < III < IV, lateral fringing and webbing absent, tips of toes II–IV moderately expanded (character state C), tip of toe I unexpanded, toe V desiccated. Inner metatarsal tubercle elongated, outer metatarsal tubercle ovoid. Tarsal fold extending 1/3 of tarsus length, from the inner metatarsal tubercle towards the heel. Subarticular tubercles nearly rounded or subconical, supernumerary tubercles nearly rounded. Measurements (in mm): SVL 23.6, HL 7.9, HW 8.4, ED 2.1, TD 1.5, EN 1.8, IND 2.1, HAL 4.8, TL 9.8, THL 10.0, FL 10.8.

Snout tip with a faded white coloration (coincident with the fleshy ridge). Blotches on the upper lip off-white. Postcommissural gland pale yellow. Tympanum light brown. Dorsal surfaces of body and limbs brown, lighter on forelimbs and heel region, digits of hand off-white. Anastomotic blotches on dorsum blackish brown; transverse bars and blotches on limbs blackish brown. Posterior surface of thigh finely mottled in shades of brown and yellow, paracloacal gland pale

yellow. Dorsolateral stripe absent, an indication of mid-dorsal, longitudinal line light grey, fragmented and restricted to the pelvic region. Ventral surface of belly and thigh partially translucent, yellowish cream. Off-white blotches on lower jaw and chest. Throat finely mottled, belly immaculate. Underside of forearm dark brown. Tubercles partly pigmented, grey, tips of fingers and toes non-pigmented.

Colour of holotype in life (Fig. 10C–D): Dorsum covered with anastomotic blotches blackish brown on a brown background. Iris golden. Tympanum brown, an orange coloration partly surrounding the tympanic annulus. Arms and legs with transverse stripes and blotches dark brown. Mid-dorsal longitudinal stripe and postcommissural gland pale yellow and dark brown. Flank finely mottled, greyish brown; glands yellow. Throat and chest brown-spotted on a partly translucent violet background, lower jaw covered with white spots, belly cream-coloured, immaculate. Underside of limbs partly translucent; outer surface of forearm dark brown with a medial, poorly delimited stripe, off-white, hindlimbs translucent, bright orange on anterior and posterior surfaces, and groin, underside of thigh granular, pale yellow.

Variation in type specimens: The female INPA-H 40515 has snout shape rounded in dorsal and lateral views and paracloacal gland absent. The male CZPB-AA 2118 has tip of toe IV fully expanded (character state D). Dorsal surfaces of body and limbs lighter brown in both paratypes.

Advertisement call: Description based on calls of two males (N = 18 notes and 70 pulses quantified; Table 3). The call (Figs 5I, 6I, 7I) consists of a single-note signal given at a rate of 52–59 (55 ± 5; N = 2) per minute. Notes are formed by 3–5 (4 ± 1) partly fused pulses given at a rate of 39–89 (68 ± 16) per second and varying in duration from 7–51 (21 ± 2) ms. Note duration varies from 66–89 (82 ± 7) ms and note rise time from 5–63 (35 ± 29)% of note duration. The note frequencies are harmonically structured and the dominant frequency may coincide either with the fundamental harmonic (1873–2003, 1926 ± 61 Hz, N = 1 male) or with the second harmonic (4055–4430, 4223 ± 171 Hz, N = 1 male). Frequency modulation is upward, rising to 43–375 (206 ± 67) Hz.

Habitat and natural history: A. tapajonica is rarely recorded in the field. The species inhabits non-flooded primary forests on the west bank of the middle-lower Tapajós River. At the type locality, a single male (holotype) was collected during the rainy season (December), while calling on the leaf litter next to the base of a terrestrial palm tree. The female was collected from a pitfall trap. At Juruti, a few males of *A. tapajonica* were observed calling sparsely on the leaf litter in plateau areas of an old-growth non-flooded forest around sunset time. *A. tapajonica* was found sympatrically with two other *Adenomera* species (*A. andreae* and *A. hylaedactyla*) at the Juruti site.

Distribution: A. tapajonica is known from the type locality and a second nearby locality on the west bank of the middle Tapajós River, and from the Juruti site (near Igarapé Mutum) located in the intervening swathe of land between the Amazon River and the lower Tapajós River (Fig. 2A).

ADENOMERA GRIDIPAPPI, SP. NOV.

GRIDI-PAPP'S TERRESTRIAL NEST-BUILDING FROG

(FIGS 2A, 3–4, 5J, 6J, 7J, 10E–F, 12E–F; TABLES 1-3)

lsid urn:lsid:zoobank.org:act:0F9B3F8A-DE7D-4680-9F72-315A74C93F64

Holotype: INPA-H 40512 (field #APL 19992), adult male, BRAZIL, Rondônia, Porto Velho, 9.414418°S, 64.429558°W, 121 m, 9-xi-2013, A.P. Lima (Collector).

Paratypes: INPA-H 40511, 40513–40514 (field #APL 19984, 19993, 21136, respectively), CFBH 44470–44472 (field #APL 21175, 21797, 21799, respectively), adult males, collected at the type locality between 2013–2016, A.P. Lima (Collector).

Referred specimens: Genetic vouchers assigned to the clade G3 of the lineage *Adenomera* sp. G of Fouquet *et al.* (2014) from the north-west portion of the Brazilian state of Mato Grosso (PMJ08, PMJ154, #968179).

Additional material: MZUSP 80593, 80595–96, 87830 (adult males), and MZUSP 80592, 80594 (adult females): BRAZIL, Mato Grosso, Aripuanã, MZUSP 151906 (adult female): BRAZIL, Mato Grosso, Juína.

Etymology: The specific epithet is a patronymic name for Marcos Gridi-Papp for his invaluable research efforts to advance the knowledge on the anuran vocal system from a functional evolutionary perspective. The honoured scientist trained the leading author of this study in acoustics and vocal anatomy during his Ph.D. program and as part of his current project dedicated to understanding the diversity and patterns of evolution of the acoustic mating signals in leptodactylid frogs. The acoustic characterization of *Adenomera* frogs has been

instrumental to elucidate the species diversity of the genus.

Diagnosis: A. gridipappi is characterized by the following combination of character states: (1) large size (adult male SVL = 25.4–27.7 mm); (2) robust body shape; (3) toe tips fully expanded into small discs (character state D); (4) distal antebrachial tubercle on underside of forearm; (5) belly immaculate; (6) two possible chromotypes (presence/absence) of dorsolateral stripe; (7) multi-note advertisement call composed of two- to four-note calls; (8) call notes formed by 2–4 partly fused pulses; (9) note duration varying from 50–75 ms; (10) note dominant frequency coinciding with the second harmonic (3553–4027 Hz); and (11) fundamental frequency ranging from 1820–1970 Hz.

Comparisons with congeners: A. gridipappi (SVL = 25.4–27.7 mm; Table 2) has adult males larger than those of *A. ajurauna, A. amicorum, A. araucaria, A. aurantiaca, A. engelsi, A. inopinata, A. kayapo, A. kweti, A. nana* and *A. phonotriccus* [combined SVL 15.4–24.0 mm (Kwet, 2007; Berneck *et al.*, 2008; Kwet *et al.*, 2009; Carvalho *et al.*, 2019b, c)]. *A. gridipappi* has a robust body shape (Fig. 12E–F), whereas *A. diptyx, A. martinezi* and *A. saci* have a slender body. *A. gridipappi* has toe tips that are fully expanded into small discs (character state D), differing from congeners with unexpanded, slightly or moderately expanded toe tips (character states A–C) as in *A. bokermanni, A. coca, A. diptyx, A. hylaedactyla, A. martinezi, A. saci* and *A. thomei*. *A. gridipappi* is distinguished from congeners (except *A. amicorum, A. aurantiaca, A. cotuba, A. inopinata, A. kayapo, A. lutzi, A. phonotriccus* and *A. tapajonica*) by having an antebrachial tubercle on underside of forearm. *A. gridipappi* differs from *A. araucaria, A. bokermanni, A. heyeri, A. kweti, A. lutzi* and *A. nana* by having belly cream-coloured (Fig. 10F), this is yellow or sometimes has yellowish tints in the other species. *A. gridipappi* is larger than its nearest relative *A. tapajonica* (Table 2) and can have a dorsolateral stripe (never present in *A. tapajonica*); however, they are more easily distinguished by their calls.

A. gridipappi can be distinguished from all congeners, either with multi-note and single-note calls (Table 3), by its unique calling emission pattern: multi-note calls are made up of two- to four-note calls (Fig. 5J)—multi-note calls of all other *Adenomera* species are composed of individual notes (Fig. 5). The other five *Adenomera* species with multi-note calls are *A. amicorum* (Fig. 5E), *A. aurantiaca* (Fig. 5G), *A. cotuba* (Fig. 5B), *A. inopinata* (Fig. 5H) and *A. simonstuarti* (T.R. de Carvalho, pers. obs.). *A. gridipappi* is also distinguished from *A. aurantiaca* (Figs 6G, 7G) and *A. inopinata* (Figs 6H, 7H), which have call notes formed by complete pulses, by having call notes formed by partly fused pulses (Figs 6J, 7J). *A. gridipappi* is distinguished from *A. amicorum* and *A. cotuba* by the shorter note duration and/or fewer pulses per note (Table 3). *A. gridipappi* can only be acoustically distinguished from *A. simonstuarti* by its unique emission pattern of multi-note calls composed of two- to four-note calls (multi-note calls of *A. simonstuarti* are composed of individual notes; T.R. de Carvalho, pers. obs.).

Description of holotype (Fig. 12E–F): Body robust. Snout subovoid to rounded in dorsal view, acuminate in lateral view. Nostril closer to the snout tip than to the eye, fleshy ridge on snout tip, canthus rostralis not marked, loreal region slightly concave, supratympanic fold from the posterior corner of the eye to the base of the arm, postcommissural gland ovoid, vocal sac subgular with a fold from jaw extending to forearm, vocal slit present, vomerine teeth in two straight rows medial and posterior to choanae and oblique to sagittal plane. Tongue elongated, free from the posterior half. Relative finger lengths IV < I < II < III, fingers without ridges or fringes, finger tips rounded, slightly expanded, especially in fingers I and V, inner metacarpal tubercle ovoid, outer metacarpal tubercle nearly rounded. Subarticular tubercles nearly rounded to subconical, supernumerary tubercles rounded. Antebrachial tubercle on underside of forearm rounded, single. Dorsum glandular, flank warty. Dorsal surface of shank and posterior surface of tarsus with white-tipped tubercles. Ventral surface of body and limb mostly smooth, underside of thigh areolate/granular. Posterior surface of thigh with ovoid paracloacal gland. Relative toe lengths I < II < V < III < IV, lateral fringing and webbing absent, tips of toes II–IV fully expanded (character state D), tip of toe I unexpanded, tip of toe V slightly expanded. Inner and outer metatarsal tubercles ovoid. Tarsal fold extending 2/3 of tarsus length, from the inner metatarsal tubercle towards the heel. Subarticular tubercles nearly rounded, supernumerary tubercles nearly rounded. Measurements (in mm): SVL 26.7, HL 8.1, HW 9.7, ED 1.9, TD 1.5, EN 1.9, IND 2.4, HAL 5.6, TL 12.4, THL 11.6, FL 12.9.

Snout tip with a faded white coloration (coincident with the fleshy ridge). Blotches on the upper lip off-white. Postcommissural gland pale yellow. Tympanum light brown. Dorsum freckled brown, lighter on limbs. Interorbital bar dark brown, outlined by a light greyish brown line, dark brown blotches and stains on dorsum, blackish brown spot coinciding with the lumbar gland. Transverse bars and blotches on

limbs dark brown. Flank finely light-brown mottled on a light grey background. Posterior surface of thigh finely mottled in shades of brown and yellow. Mid-dorsal longitudinal line and dorsolateral stripe absent. Posterior surface of thigh cream-coloured and covered with brown spots and dots. Paracloacal gland pale yellow. Ventral surface of belly and limbs partially translucent, cream-coloured. Throat brown-dotted, more densely coloured laterally, chest and belly immaculate. Underside of forearm (outer margin) brown-speckled, ventral surface of hand, foot and digits mostly brown interspersed with lighter sections, subarticular tubercles partly pigmented, light grey, and tips of fingers and toes non-pigmented.

Variation in type specimens: Dorsal coloration varies from light brown to dark solid blackish brown. Dorsolateral stripe (light grey) present in CFBH 44470. Mid-dorsal longitudinal stripe, restricted to pelvic region, present in CFBH 44470-71. Shape and size of antebrachial tubercles are variable among type specimens, sometimes low and flattened (hardly detected even under magnification). Variation in toe tip development of toes II–IV varies from modestly expanded to fully expanded (character states C and D, respectively). The holotype was not photographed in life, but colours in life of a paratype are shown in Fig. 10E–F.

Advertisement call: Description based on calls of four males (N = 73 notes and 250 pulses quantified; Table 3). The call (Figs 5J, 6J, 7J) consists of pulsed notes grouped into two levels of temporal organization: two-note (*c*. 75% of calls), three-note (*c*. 25%) and four-note (a single case) calls that are given in bouts (4–8, 5 ± 1 calls per bout; N = 13). The only exception was the emission of single-note calls at the beginning of a call bout (= multi-note call) given by one male. Multi-note calls are composed of 9–16 (12 ± 3; N = 13) notes given at a rate of 2–3 (3 ± 1; N = 4) per second. Notes are formed by 2–4 (3 ± 1) partly fused pulses given at a rate of 35–98 (68 ± 11) per second and varying in duration from 8–40 (21 ± 4) ms. Note duration varies from 50–75 (64 ± 8) ms and note rise time from 7–74 (42 ± 4)% of note duration. The note frequencies are harmonically structured and the dominant frequency coincides with the second harmonic (3553–4027, 3856 ± 105 Hz). The note fundamental frequency ranges from 1820–1970 (1887 ± 13) Hz. Frequency modulation is upward, when present, ranging from 0–732 (342 ± 52) Hz.

Habitat and natural history: Males were heard calling hidden under the leaf litter of an old-growth non-flooded forest during the daytime at the onset of rainy season (November and December). No individual was recorded in calling activity in the rainy season later than early January. *A. andreae* and *A. hylaedactyla* are sympatric congeners with *A. gridipappi* at the type locality.

Distribution: A. gridipappi is distributed in the interfluvial region delimited by the upper Madeira and Aripuanã rivers, in southern Brazilian Amazonia (Fig. 2A).

Remarks: Genetic vouchers associated with lineage sp. G from the lower Madeira and Tapajós rivers still require acoustic data for a precise taxonomic assessment. Specimens from Borba [genetic vouchers MTR 12832 (MZUSP 158074) and MTR 12900 (without an associated museum number)] formed a clade with the type series of *A. gridipappi*; however, we do not have associated calls that could confirm that they are conspecific to each other. Besides, these populations are separated geographically by almost 800 km and genetic divergence in *COI* coincides with the 5% threshold of interspecific variation defined in our species delimitation analysis (Table 1). Until additional data are obtained, we provisionally assign both genetic vouchers from Borba to *A.* cf. *gridipappi*. All four genetic vouchers from Nova Olinda do Norte [MTR 12711 (MZUSP 158073) and MTR 13034, 13067, SMS 639 (without associated museum numbers)] form a clade sister of *A. gridipappi* + *A. tapajonica* with full support in our analyses (Fig. 3; Supporting Information, Fig. S2). These two new sister species are categorically distinguished from each other based on their calls, whereas minor differences in morphology and coloration did not help much to their discrimination. We only had access to one genetic voucher of the 'Nova Olinda do Norte lineage', an adult female that shares phenotypic traits with both *A. gridipappi* and *A. tapajonica*, and calls from this lineage remain unknown. Therefore, we refrain from naming the Nova Olinda do Norte lineage as a new species while acoustic data can be acquired. For that reason, we provisionally assign it to *Adenomera* sp. of the *A. heyeri* clade. It is noteworthy that one of the genetic vouchers of *Adenomera* sp. and one of *A.* cf. *gridipappi* were collected from opposite margins of the Abacaxis River, and the collection points are separated one from the other by less than 5 km. Based on the interfluve-associated species distributions in the *A. heyeri* clade, this could be a piece of evidence pointing to the existence of two unnamed species on opposite river banks (*A.* cf. *gridipappi* and *Adenomera* sp.) associated with the Abacaxis River, a tributary of the Amazon River in the Madeira-Tapajós interfluve. If true, this would be a case similar to that of the nearest relatives and assumedly allopatric *A. aurantiaca* and *A. inopinata*, distributed on opposite banks of another

smaller river (Jamanxim River) in the Amazon Basin (Fig. 2B).

DISCUSSION

The use of multiple lines of evidence, mainly the combination of morphological, acoustic and molecular data, has been increasingly and successfully used to define the taxonomic status of various groups of frogs, notably in *Adenomera* (e.g. Carvalho *et al.*, 2019a, b; Cassini *et al.*, 2020). Advertisement call patterns in the *A. heyeri* clade were found to be much more diverse than previously known, which endorse the high taxonomic value of acoustic data for the assessment of species diversity of *Adenomera* frogs. Two (sp. F and sp. G) of the four candidate new species within the *A. heyeri* clade of Fouquet *et al.* (2014) were split into six new species in the present study, besides a seventh species recently described as *A. phonotriccus* (Carvalho *et al.*, 2019c) and an eighth possibly unnamed species (*Adenomera* sp.; Table 1; Fig. 3). Some of these were in fact assumed in Fouquet *et al.* (2014), who found concordance between additional mitochondrial DNA subdivision and nuclear DNA. Our results confirm the assumption that their species delimitation was overconservative in many instances.

The morphology (e.g. antebrachial tubercle and SVL), colouration (e.g. dorsolateral stripe, belly and thigh colour patterns) and calls (e.g. pulsed vs. non-pulsed and single-note vs. multi-note calls) resulted in unique combinations of phenotypic traits among closely related species across the *A. heyeri* clade. Of these there are three species for which intraspecific variation could not be appropriately assessed in our study given their rarity and lack of integrated information for the accurate taxonomic assessment of specimens morphologically examined (i.e. direct association of specimens with calls and DNA sequences; Supporting Information, Appendix S1): *A. aurantiaca*, *A. inopinata* and *A. tapajonica*. There are three main reasons by which we decided to describe these three lineages as new species. First, the recognition and description of the species are supported by multiple lines of evidence, i.e. acoustic (call emission patterns, pulsing type and call rise time), molecular (phylogenetic relationships and *COI* distances ≥ 8%) and morphological (SVL and thigh colour patterns) data, when compared to each other and to other members of the *A. heyeri* clade (Tables 1, 2, 3; Figs 3, 5–7, 9–12). Second, major patterns of advertisement call within *Adenomera* have shown to be diverse across species but generally stereotyped within species (e.g. Angulo *et al.*, 2003; Kwet, 2007; Carvalho & Giaretta, 2013 a, b; Carvalho *et al.*, 2019c, b), therefore are a reliable source of information for taxonomic decision making in this frog genus. Third, according to the recommendation of Carvalho *et al.* (2019d), the potential extinction risk of rare and/or patchily distributed species of Amazonian *Adenomera* far outweighs that of eventual synonymization of any of them, which currently appears unlikely to happen based on the given evidence.

The lineage of 'sp. F' was previously indicated as comprising three major clades [F1–F3 (Fouquet *et al.*, 2014)]. All three clades in sp. F are now associated with species names: *A. kayapo* (= F1), *A. amicorum* (= F2) and *A. phonotriccus* [= F3 (Carvalho *et al.*, 2019c)]. The morphologically cryptic and closest related *A. phonotriccus* and *A. kayapo* have sympatric occurrence at a single location in the Xingu-Tocantins interfluve, whereas the allopatric *A. amicorum* is distributed in the Tapajós-Xingu interfluve (Fig. 2B). The lineage of 'sp. G' was previously indicated as comprising four major clades [G1–G4 (Fouquet *et al.*, 2014)]. Based on phylogenetic relationships (Fig. 3) and high divergence in *COI* (Table 1), the clades G1 and G4 probably correspond to additional undescribed species assigned here as *Adenomera* sp. due to lack of morphological or acoustic evidence. Clade G2 was assigned to *A.* cf. *gridipappi*, given the lack of any other evidence to confirm its taxonomic identity, and clade G3 corresponds to one of the species described herein as new (*A. gridipappi*). In addition to these, three other lineages with affinities to sp. G were named in the present study (*A. aurantiaca*, *A. inopinata* and *A. tapajonica*). Lineages previously assigned to sp. G were found to be distributed in two Amazonian interfluves (Madeira-Tapajós and Tapajós-Xingu; Fig. 2). In contrast to species within sp. F (*A. phonotriccus* and *A. kayapo*) and *A. cotuba*-*A. juikitam*, species allied to sp. G lineages were never found in sympatry with each other.

To our knowledge, the distributions of *A. cotuba* and *A. juikitam* are limited by the Araguaia River. Both species have westernmost occurrence points precisely on the east margin of the Araguaia River (Fig. 1B). The opposite (west) margin of the Araguaia River corresponds to easternmost occurrence points of *A. phonotriccus* (Fig. 2B), whereas *A. kayapo* is distributed on both sides of the Araguaia River. *Adenomera cotuba* and *A. juikitam* are mostly associated with the DD, but also occur in the Cerrado-Amazonia ecotone (Fig. 1B), occupying savanna and dry forest habitats, whereas *A. kayapo* and *A. phonotriccus* occupy Amazonian non-flooded forests although *A. kayapo* is also distributed to the south in the Cerrado-Amazonia ecotone (Fig. 2B). According to the phylogenetic relationships and historical biogeography of the *A. heyeri* clade, cases of sympatry among these species should reflect distinct scenarios. *Adenomera juikitam* is distantly related to *A. cotuba*, representing the most ancient

cladogenesis in the clade and the first dispersal from northern Amazonia (Guiana Shield) to the DD (Fig. 4; Supporting Information, Fig. S2), whereas the lineage of *A. cotuba* separated more recently, coinciding with the second dispersal event from Amazonia (Tapajós-Xingu interfluve in the southern Amazon Basin) to the DD (Fig. 4; Supporting Information, Fig. S2). The subsequent expansion of the geographic ranges of these species may have generated secondary contact of these morphologically and acoustically divergent species (Figs 1B, 4). *A. kayapo* and *A. phonotriccus*, on the other hand, are sister taxa with cryptic morphology, but have markedly divergent advertisement calls, and their syntopic occurrence might be explained either by sympatric/parapatric speciation or by secondary contact (Figs 2B, 4). The sympatric occurrence of *A. kayapo* and *A. juikitam* in the Cerrado-Amazonia ecotone should also reflect geographic range expansion of these distantly related lineages of the *A. heyeri* clade between the DD and the Xingu-Tocantins interfluve leading to secondary contact (Figs 1B, 2B, 4).

Our study revealed many candidate new species across Brazilian Amazonia, six of them formally named and described. Data on distribution and local abundances of these species are scanty, preventing us from accurately assessing the potential extinction risks associated with each of the six newly described *Adenomera* species. Species distributions appear in almost all cases to be delimited by interfluves, but we are unaware whether they are widely distributed throughout an interfluvial area or might be narrow endemics to the river banks within these areas (Fig. 2). A major limitation is the lack of information on distribution range and potential rarity of some species (e.g. *A. inopinata*). Therefore, it is important to highlight that the current state of knowledge on species of the *A. heyeri* clade is likely biased by insufficient sampling in central interfluvial areas, which are, in many instances, hard-to-access and isolated locations (see Oliveira *et al.*, 2016). *Adenomera cotuba* and *A. juikitam*, on the other hand, are widely distributed and relatively abundant across the north-central portion of the DD and the Cerrado-Amazonia ecotone (Fig. 1B), and thus they could be classified in the Least Concern category (*sensu* IUCN, 2012).

Members across the major clades of *Adenomera* share a recurrent pattern of cryptic morphology; however, closely related species in the genus generally differ markedly in their calls (e.g. Angulo *et al.*, 2003; Carvalho & Giaretta, 2013b; Carvalho *et al.*, 2019b). This is a general rule in the *A. heyeri* clade: the three closest related species previously subsumed within *Adenomera* sp. F (*A. kayapo*, *A. amicorum* and *A. phonotriccus*) have highly divergent calls (Figs 5–7) by their distinct pulsing (incomplete vs. complete) and temporal organization (single-note vs. multi-note), rendering them categorically distinct to each other from an acoustic perspective. Pronounced acoustic divergence can also be observed among newly described species previously subsumed within *Adenomera* sp. G or with affinities to this lineage (e.g. *A. tapajonica* and *A. gridipappi*). Both species distributed in the DD (*A. cotuba* and *A. juikitam*), distantly related and partly sympatric with each other, also acquired distinct call patterns (multi-note and single-note calls, respectively, Fig. 5B–C). Additional cases of acoustic differentiation in pulsing and/or temporal organization have also been reported between closely related species of other *Adenomera* clades (Angulo & Icochea, 2010; Carvalho & Giaretta, 2013b; Carvalho *et al.*, 2019d). The repeated acquisition of certain call patterns within *Adenomera* is a major evolutionary trend in this Neotropical frog genus, which will be well suited for future research investigating the evolutionary processes promoting the convergent evolution of acoustic mating signals.

Dispersal events from Amazonia to the DD occurred three times independently in the diversification of *Adenomera*, twice in the *A. heyeri* clade (Fig. 4) and a third time in the lineage splitting of the 'open-formation clade', i.e. *A. hylaedactyla*+*A. martinezi* clades (see Fouquet *et al.*, 2014). Historical connections between the Guiana Shield and the Brazilian Shield (including the DD) and biotic diversification associated with these possible routes are known for other vertebrates (Silva & Bates, 2002; Quijada-Mascareñas *et al.*, 2007; Leite *et al.*, 2015). Two connection routes (*sensu* Silva & Bates, 2002; Quijada-Mascareñas *et al.*, 2007) appear to have been used as dispersal routes in the *A. heyeri* clade: a central route between the Guiana Shield and the Brazilian Shield through the 'low precipitation belt' (Silva, 1995) may have accounted for the most recent origin of the lineages distributed south of the Amazon River and *A. cotuba* in the DD. Another route between the eastern Guiana Shield and northeast portion of the DD might have been used by the early-splitting *A. juikitam*. However, we cannot rule out biased results generated by the putative extinction of ancestral taxa when we look at the old divergence time (15.8 Mya) between *A. juikitam* and the remaining lineages of the *A. heyeri* clade (Supporting Information, Fig. S2).

Overall, our results indicate that lineage diversification within the *A. heyeri* clade across the southern tributaries of the Amazon River (Fig. 4; Supporting Information, Fig. S2) is more recent than the period of establishment of the transcontinental Amazon River system [*c.* 10 Mya (Hoorn *et al.*, 2010)]. Diversification within this frog clade must have resulted from dispersal events from northern Amazonia to the DD and interfluvial regions south of the Amazon River. However, our results do not rule out the possibility that the major southern tributaries of the Amazon River act (or have acted) as geographic

barriers limiting dispersal (see Pirani *et al.*, 2019). Interfluves in the southern Amazon Basin can contribute as secondary diversification agents or geographic filters for dispersal and establishment of taxa rather than a primary role causing vicariant speciation (Moraes *et al.*, 2016; Maia *et al.*, 2017). The currently known distribution ranges of the newly described species and related candidate new species of the *A. heyeri* clade are likely maintained by the major southern tributaries of the Amazon River (Fig. 2), whereas the two members from northern Amazonia (*A. heyeri* and sp. Q) are seemingly restricted in the south by the main course of the Amazon River (Fig. 1A). This pattern could indicate a relevant role of these well-known historical barriers to biotic dispersal and drivers of vicariant speciation (Dias-Terceiro *et al.*, 2015; Moraes *et al.*, 2016; Silva *et al.*, 2019) in the diversification of this frog clade. Because some members of the genus *Adenomera* appear to be strongly associated with distinct vegetation types or ecoregions, the *A. heyeri* clade may also have been especially susceptible to climate instability in eastern Amazonia during more recent periods, when changes in the composition and extent of forest and dry habitats have occurred in the region (Cheng *et al.*, 2013; Wang *et al.*, 2017). The historical biogeography of this clade of South American frogs constitutes an additional piece of evidence supporting that the river-barrier hypothesis is not universally applied to the dynamic picture of diversification processes shaping the evolutionary history of the extant biota of Amazonia.

ACKNOWLEDGMENTS

Financial support was received through research grants from São Paulo Research Foundation (Fundação de Amparo à Pesquisa do Estado de São Paulo; FAPESP grant #2013/50741-7) and the National Council for Scientific and Technological Development (Conselho Nacional de Desenvolvimento Científico e Tecnológico; CNPq grants #446935/2014-0, #313055/2015-7, and #306623/2018-8). T.R.C. has received from FAPESP a postdoctoral fellowship (#2017/08489-0) and visiting research fellowships (#2015/13404-8 and #2018/17118-8). M.T.R. thanks FAPESP (grants #2003/10335-8 and #2011/50146-6) and CNPq. Fieldwork by P.L.V.P. was supported by a grant from the Fresno Chaffee Zoo Wildlife Conservation Fund collecting permits were granted by Instituto Chico Mendes de Conservação da Biodiversidade (ICMBio/SISBIO #30059, #38143-2) and Instituto Brasileiro do Meio Ambiente e dos Recursos Naturais Renováveis (IBAMA #1081/2011, IBAMA #066/2012, IBAMA #903/2018). We are grateful to Centro de Estudo de Insetos Sociais (CEIS) and Mariana L. Lyra for providing lab space and technical expertise in DNA sequencing protocols. Special thanks to Albedi Andrade Jr., Ana B. Barros, Bernardo F. V. Teixeira, Cyro S. Bernardes, Elizângela S. Brito, Felipe Curcio, Francisco dal Vechio, Gabriela R. Gonçalves, Igor J. Roberto, Ivan Prates, Jerriane O. Gomes, José Cassimiro, José M. Guellere, Leandro A. Silva, Lucas B. Martins, Luis Storti, Marcelo J. Sturaro, Marco Sena, Mauro Hoffman, Mauro Teixeira Jr., Pablo V. Cerqueira, Pedro Marinho, Priscila S. Carvalho, Renato Recoder, Sérgio Marques-Souza, Silvia Pavan and Tainá F. D. Rodrigues for their companionship during field expeditions and/or for making available morphological and acoustic data and photographs. We also thank Arcadis-Logos and CNEC WorleyParsons Engenharia S.A. for logistical and/or financial support during field expeditions to the Jirau/Belo Monte power plants and middle Tapajós River region. Many thanks also to the following individuals for providing access to specimens under their care for morphological work: Ana L.C. Prudente and Fabricio Sarmento (MPEG), Fernanda P. Werneck and Ariane Silva (INPA-H), Nadya Pupin (CFBH), L. Felipe Toledo and Karina Rabelo (ZUEC), Marcelo Menin (CZPB-AA), Taran Grant and Aline S. Benetti (MZUSP), Glaucia F. Pontes (MCP), Paulo C.A. Garcia (UFMG), Marcelo N.C. Kokubum (LHUFCG), Robson W. Ávila and Igor J. Roberto (URCA-H) and César Aguilar-Puntriano (MUSM). The Fonoteca Neotropical Jacques Vielliard (FNJV) and the Macaulay Library at the Cornell Lab of Ornithology (ML) enabled access to *Adenomera* sound files.

REFERENCES

Almeida AP, **Angulo A. 2006.** A new species of *Leptodactylus* (Anura: Leptodactylidae) from the state of Espírito Santo, with remarks on the systematics of associated populations. *Zootaxa* **1334:** 1–25.

Angulo A, **Icochea J. 2010.** Cryptic species complexes, widespread species and conservation: lessons from Amazonian frogs of the *Leptodactylus marmoratus* group (Anura: Leptodactylidae). *Systematics and Biodiversity* **8:** 357–370.

Angulo A, **Reichle S. 2008.** Acoustic signals, species diagnosis, and species concepts: the case of a new cryptic species of *Leptodactylus* (Amphibia, Anura, Leptodactylidae) from the Chapare Region, Bolivia. *Zoological Journal of the Linnean Society* **152:** 59–77.

Angulo A, **Cocroft RB**, **Reichle S. 2003.** Species identity in the genus *Adenomera* (Anura: Leptodactylidae) in southeastern Peru. *Herpetologica* **59:** 490–504.

Antonelli A, **Zizka A**, **Carvalho FA**, **Scharn R**, **Bacon CD**, **Silvestro D**, **Condamine FL. 2018.** Amazonia is the primary source of Neotropical biodiversity. *Proceedings of the National Academy of Sciences of the United States of America* **115:** 6034–6039.

Audacity Team. 2017. *Audacity(R): free audio editor and recorder, version 2.2.1*. Available at: https://www.audacityteam.org

Azevedo-Ramos C, Galatti U. 2002. Patterns of amphibian diversity in Brazilian Amazonia: conservation implications. *Biological Conservation* **103:** 103–111.

Batalha-Filho H, Fjeldså J, Fabre PH, Miyaki CY. 2013. Connections between the Atlantic and the Amazonian forest avifaunas represent distinct historical events. *Journal of Ornithology* **154:** 41–50.

Berneck BVM, Costa COR, Garcia PCA. 2008. A new species of *Leptodactylus* (Anura: Leptodactylidae) from the Atlantic Forest of São Paulo State, Brazil. *Zootaxa* **1795:** 46–56.

Boettger O. 1885. Liste von Reptilien und Batrachiern aus Paraguay. *Zeitschrift für Naturwissenschaften* **58:** 213–248.

Boistel R, Massary GC, Angulo A. 2006. Description of a new species of the genus *Adenomera* (Amphibia, Anura, Leptodactylidae) from French Guyana. *Acta Herpetologica* **1:** 1–14.

Bokermann WCA. 1956. Sôbre una nueva especie de *Leptodactylus* del Brasil (Amphibia). *Neotropica* **2:** 37–40.

Bouckaert R, Heled J, Kühnert D, Vaughan T, Wu C-H, Xie D, Suchard MA, Rambaut A, Drummond AJ. 2014. BEAST 2: a software platform for Bayesian evolutionary analysis. *PLoS Computational Biology* **10:** e1003537.

Carvalho TR, Angulo A, Kokubum MNC, Barrera DA, Souza MB, Haddad CFB, Giaretta AA. 2019a. A new cryptic species of the *Adenomera andreae* clade from southwestern Amazonia (Anura: Leptodactylidae). *Herpetologica* **75:** 233–246.

Carvalho TR, Giaretta AA. 2013a. Bioacoustics reveals two new syntopic species of *Adenomera Steindachner* (Anura: Leptodactylidae: Leptodactylinae) in the cerrado of central Brazil. *Zootaxa* **3731:** 533–551.

Carvalho TR, Giaretta AA. 2013b. Taxonomic circumscription of *Adenomera martinezi* (Bokermann, 1956) (Anura: Leptodactylidae: Leptodactylinae) with the recognition of a new cryptic taxon though a bioacoustic approach. *Zootaxa* **3701:** 207–237.

Carvalho TR, Cassini CS, Taucce PPG, Haddad CFB. 2019b. A new, morphologically cryptic species of *Adenomera* closely related to *A. araucaria* from the Atlantic Forest of southern Brazil (Anura, Leptodactylidae). *Journal of Herpetology* **53:** 131–143.

Carvalho TR, Giaretta AA, Angulo A, Haddad CFB, Peloso PLV. 2019c. A new Amazonian species of *Adenomera* (Anura: Leptodactylidae) from the Brazilian state of Pará: a tody-tyrant voice in a frog. *American Museum Novitates* **3919:** 1–21.

Carvalho TR, Giaretta AA, Maciel NM, Barrera DA, Aguilar-Puntriano C, Haddad CFB, Kokubum MNC, Menin M, Angulo A. 2019d. On the uncertain taxonomic identity of *Adenomera hylaedactyla* (Cope, 1868) and the composite type series of *A. andreae* (Müller, 1923) (Anura, Leptodactylidae). *Copeia* **107:** 708–723.

Cassini CS, Taucce PPG, de Carvalho TR, Fouquet A, Solé M, Haddad CFB, Garcia PCA. 2020. One step beyond a broad molecular phylogenetic analysis: species delimitation of *Adenomera marmorata* Steindachner, 1867 (Anura: Leptodactylidae). *PLoS One* **15:** e0229324.

Cheng H, Sinha A, Cruz FW, Wang X, Edwards RL, d'Horta FM, Ribas CC, Vuille M, Stott LD, Auler AS. 2013. Climate change patterns in Amazonia and biodiversity. *Nature Communications* **4:** 1411–1416.

Clark K, Karsch-Mizrachi I, Lipman DJ, Ostell J, Sayers EW. 2016. GenBank. *Nucleic Acids Research* **44:** D67–D72.

Cope ED. 1868. An examination of the Reptilia and Batrachia obtained by the Orton Expedition to Equador and the upper Amazon, with notes on other species. *Proceedings of the Academy of Natural Sciences of Philadelphia* **20:** 96–140.

Costa LP. 2003. The historical bridge between the Amazon and the Atlantic forest of Brazil: a study of molecular phylogeography with small mammals. *Journal of Biogeography* **30:** 71–86.

Cracraft J. 1985. Historical biogeography and patterns of differentiation within the South American avifauna: areas of endemism. *Ornithological Monographs* **36:** 49–84.

Dagosta FCP, de Pinna M. 2017. Biogeography of Amazonian fishes: deconstructing river basins as biogeographic units. *Neotropical Ichthyology* **15:** e170034.

De Queiroz K. 2007. Species concepts and species delimitation. *Systematic Biology* **56:** 879–886.

Dias-Terceiro RG, Kaefer IL, Fraga R, Araújo MC, Simões PI, Lima AP. 2015. A matter of scale: historical and environmental factors structure anuran assemblages from the upper Madeira River, Amazonia. *Biotropica* **47:** 259–266.

Drummond AJ, Ho SY, Phillips MJ, Rambaut A. 2006. Relaxed phylogenetics and dating with confidence. *PLoS Biology* **4:** e88.

Feng YJ, Blackburn DC, Liang D, Hillis DM, Wake DB, Cannatella DC, Zhang P. 2017. Phylogenomics reveals rapid, simultaneous diversification of three major clades of Gondwanan frogs at the Cretaceous-Paleogene boundary. *Proceedings of the National Academy of Sciences of the USA* **114:** 5864–5870.

Fernandes AM, Cohn-Haft M, Hrbek T, Farias IP. 2014. Rivers acting as barriers for bird dispersal in the Amazon. *Revista Brasileira de Ornitologia* **22:** 363–373.

Fitzinger LJFJ. 1826. *Neue Classification der Reptilien nach ihren natürlichen Verwandtschaften nebst einer Verwandtschafts-tafel und einem Verzeichnisse der Reptilien-sammlung des K. K. Zoologisch Museum's zu Wien*. Vienna: J. G. Heubner.

Fluck IE, Cáceres N, Hendges CD, Brum MN, Dambros CS. 2020. Climate and geographic distance are more influential than rivers on the beta diversity of passerine birds in Amazonia. *Ecography (early view)*: 1–9. Doi: 10.1111/ecog.04753

Fouquet A, Cassini CS, Haddad CFB, Pech N, Rodrigues MT. 2014. Species delimitation, patterns of diversification and historical biogeography of the Neotropical frog genus *Adenomera* (Anura, Leptodactylidae). *Journal of Biogeography* **41:** 855–870.

Frost DR, **Hillis DM. 1990.** Species concepts and practice: herpetological applications. *Herpetologica* **46:** 259–294.

Frost DR, **Crafts HM**, **Fitzgerald L**, **Titus TA. 1998.** Geographic variation, species recognition, and molecular evolution of cytochrome oxidase I in the *Tropidurus spinulosus* complex (Iguania: Tropiduridae). *Copeia* **1998:** 839–851.

Gallardo JM. 1963. *Hydrolaetare*, nuevo género de Leptodactylidae (Amphibia) neotropical. *Neotropica* **9:** 42–48.

Gernhard T. 2008. The conditioned reconstructed process. *Journal of Theoretical Biology* **253:** 769–778.

Gridi-Papp M. 2007. *Soundruler: acoustic analysis for research and teaching, version 0.9.6.1*. Available at: http://soundruler.sourceforge.net

Haffer J. 1978. Distribution of Amazon birds. *Bonner Zoologischen Beiträge* **29:** 38–78.

Heyer WR. 1973. Systematics of the *marmoratus* group of the frog genus *Leptodactylus* (Amphibia, Leptodactylidae). *Contributions in Science, Natural History Museum of Los Angeles County* **251:** 1–50.

Heyer WR. 1975. *Adenomera lutzi* (Amphibia: Leptodactylidae), a new species of frog from Guyana. *Proceedings of the Biological Society of Washington* **88:** 315–318.

Heyer WR, **Rand AS**, **Cruz CAG**, **Peixoto OL**, **Nelson CE. 1990.** Frogs of Boracéia. *Arquivos de Zoologia, Museu de Zoologia da Universidade de São Paulo* **31:** 231–410.

Hoorn C, **Wesselingh FP**, **ter Steege H**, **Bermudez MA**, **Mora A**, **Sevink J**, **Sanmartín I**, **Sanchez-Meseguer A**, **Anderson CL**, **Figueiredo JP**, **Jaramillo C**, **Riff D**, **Negri FR**, **Hooghiemstra H**, **Lundberg J**, **Stadler T**, **Särkinen T**, **Antonelli A. 2010.** Amazonia through time: Andean uplift, climate change, landscape evolution, and biodiversity. *Science* **330:** 927–931.

von Humboldt A. 1825. *Voyage aux régions équinoxiales du nouveau continent, fait en 1799, 1800, 1801, 1802, 1803 et 1804*. Paris: F. Schoell.

IUCN. **2012.** *IUCN red list categories and criteria, version 3.1, 2nd edn*. Gland and Cambridge: IUCN.

Katoh K, **Standley DM. 2013.** MAFFT multiple sequence alignment software version 7: improvements in performance and usability. *Molecular Biology and Evolution* **30:** 772–780.

Kearse M, **Moir R**, **Wilson A**, **Stones-Havas S**, **Cheung M**, **Sturrock S**, **Buxton S**, **Cooper A**, **Markowitz S**, **Duran C**, **Thierer T**, **Ashton B**, **Mentjies P**, **Drummond A. 2012.** Geneious Basic: an integrated and extendable desktop software platform for the organization and analysis of sequence data. *Bioinformatics* **28:** 1647–1649.

Kok PJR, **Kokubum MNC**, **MacCulloch RD**, **Lathrop M. 2007.** Morphological variation in *Leptodactylus lutzi* (Anura, Leptodactylidae) with description of its advertisement call and notes on its courtship behavior. *Phyllomedusa, Journal of Herpetology* **6:** 45–60.

Kumar S, **Stecher G**, **Tamura K. 2016.** MEGA7: Molecular Evolutionary Genetics Analysis version 7.0 for bigger datasets. *Molecular Biology and Evolution* **33:** 1870–1874.

Kwet A. 2007. Bioacoustic variation in the genus *Adenomera* in southern Brazil, with revalidation of *Leptodactylus nanus* Müller, 1922 (Anura, Leptodactylidae). *Mitteilungen aus dem Museum für Naturkunde in Berlin, Zoologische Reihe Supplement* **83:** 56–68.

Kwet A, **Angulo A. 2002.** A new species of *Adenomera* (Anura, Leptodactylidae) from the *Araucaria* forest of Rio Grande do Sul (Brazil), with comments on the systematic status of southern populations of the genus. *Alytes* **20:** 28–43.

Kwet A, **Steiner J**, **Zillikens A. 2009.** A new species of *Adenomera* (Amphibia: Anura: Leptodactylidae) from the Atlantic rain forest in Santa Catarina, southern Brazil. *Studies on Neotropical Fauna and Environment* **44:** 93–107.

Lanfear R, **Frandsen PB**, **Wright AM**, **Senfeld T**, **Calcott B. 2017.** PartitionFinder 2: new methods for selecting partitioned models of evolution for molecular and morphological phylogenetic analyses. *Molecular Biology and Evolution* **34:** 772–773.

Leite RN, **Rogers DS. 2013.** Revisiting Amazonian phylogeography: insights into diversification hypotheses and novel perspectives. *Organisms Diversity & Evolution* **13:** 639–664.

Leite YLR, **Kok PJR**, **Weksler M. 2015.** Evolutionary affinities of the "Lost World" mouse suggest a late Pliocene connection between the Guiana and Brazilian shields. *Journal of Biogeography* **42:** 706–715.

Ligges U, **Krey S**, **Mersmann O**, **Schnackenberg S. 2017.** *TuneR: analysis of music and speech*. Available at: https://CRAN.R-project.org/package=tuneR

Lyra ML, **Haddad CFB**, **de Azeredo-Espin AML. 2017.** Meeting the challenge of DNA barcoding Neotropical amphibians: polymerase chain reaction optimization and new COI primers. *Molecular Ecology Resources* **17:** 966–980.

Maia GF, **Lima AP**, **Kaefer IL. 2017.** Not just the river: genes, shapes, and sounds reveal population-structured diversification in the Amazonian frog *Allobates tapajos* (Dendrobatoidea). *Biological Journal of the Linnean Society* **121:** 95–108.

Márquez R, **De la Riva I**, **Bosch J. 1995.** Advertisement calls of Bolivian Leptodactylidae (Amphibia, Anura). *Journal of Zoology* **237:** 313–336.

Marty C, **Gaucher P. 1999.** *Sound guide to the tailless amphibians of French Guiana*. France: Centre Bioacoustique Alpin.

Matlab. **2004.** *The language of technical computing, version 6.5.2*. Natick: The MathWorks Inc.

Matzke NJ. 2014. Model selection in historical biogeography reveals that founder-event speciation is a crucial process in island clades. *Systematic Biology* **63:** 951–970.

Meyer CP. 2003. Molecular systematics of cowries (Gastropoda: Cypraeidae) and diversification patterns in the tropics. *Biological Journal of the Linnean Society* **79:** 401–459.

Moraes LJCL, **Pavan D**, **Barros MC**, **Ribas CC. 2016.** The combined influence of riverine barriers and flooding gradients on biogeographical patterns for amphibians and squamates in south-eastern Amazonia. *Journal of Biogeography* **43:** 2113–2124.

Müller L. 1922. Über eine Sammlung Froschlurche von Sta. Catarina nebst Beschreibung zweier neuer Arten. *Blätter für Aquarien- und Terrarien-Kunde, Stuttgart* **33:** 167–171.

Müller L. 1923. Neuer oder seltene Reptilien und Batrachier der zoologischen Sammlung des bayerischen Staates. *Zoologischer Anzeiger* **57:** 38–42.

Naka LN, **Brumfield RT. 2018.** The dual role of Amazonian rivers in the generation and maintenance of avian diversity. *Science Advances* **4:** e8575.

Oliveira JSP, **Freitas EB**, **Lima CA**, **Pires RAP**, **De-Carvalho CB. 2018.** Geographic distribution: *Adenomera cotuba*. *Herpetological Review* **49:** 69.

Oliveira U, **Paglia AP**, **Brescovit AD**, **Carvalho CJB**, **Silva DP**, **Rezende DT**, **Leite FSF**, **Batista JAN**, **Barbosa JPPP**, **Stehmann JR**, **Ascher JS**, **Vasconcelos MF**, **De Marco Jr J**, **Löwenberg-Neto P**, **Dias PG**, **Ferro VG**, **Santos AJ. 2016.** The strong influence of collection bias on biodiversity knowledge shortfalls of Brazilian terrestrial biodiversity. *Diversity and Distributions* **22:** 1232–1244.

Padial JM, **Chaparro JC**, **Castroviejo-Fisher S**, **Guayasamin JM**, **Lehr E**, **Delgado AJ**, **Vaira M**, **Teixeira Jr M**, **Aguayo R**, **De la Riva I. 2012.** A revision of species diversity in the Neotropical genus *Oreobates* (Anura: Strabomantidae), with the description of three new species from the Amazonian slopes of the Andes. *American Museum Novitates* **3752:** 1–55.

Palumbi SR, **Martin A**, **Romano S**, **Mcmillan WO**, **Stice L**, **Grabowski G. 1991.** *The simple fool's guide to PCR*. Honolulu: University of Hawaii.

Pirani RM, **Werneck FP**, **Thomaz AT**, **Kenney ML**, **Sturaro MJ**, **Ávila-Pires TCS**, **Peloso PLV**, **Rodrigues MT**, **Knowles LL. 2019.** Testing main Amazonian rivers as barriers across time and space within widespread taxa. *Journal of Biogeography* **46:** 2444–2456.

Prado DE, **Gibbs PE. 1993.** Patterns of species distributions in the dry seasonal forest South America. *Annals of the Missouri Botanic Garden* **80:** 902–927.

Puillandre N, **Lambert A**, **Brouillet S**, **Achaz G. 2012.** ABGD, Automatic Barcode Gap Discovery for primary species delimitation. *Molecular Ecology* **21:** 1864–1877.

Qian H, **Ricklefs RE. 2007.** A latitudinal gradient in large-scale beta diversity for vascular plants in North America. *Ecology Letters* **10:** 737–744.

Quijada-Mascareñas JA, **Ferguson JE**, **Pook CE**, **Salomão MG**, **Thorpe RS**, **Wüster W. 2007.** Phylogeographic patterns of trans-Amazonian vicariants and Amazonian biogeography: the Neotropical rattlesnake (*Crotalus durissus* complex) as an example. *Journal of Biogeography* **34:** 1296–1312.

Rambaut A, **Suchard MA**, **Xie D**, **Drummond AJ. 2018.** *Tracer version 1.7*. Available at: http://tree.bio.ed.ac.uk/software/tracer

R Core Team. **2018.** *R: a language and environment for statistical computing, version 3.5.0*. Vienna: R Foundation for Statistical Computing. Available at: http://www.r-project.org

Ribas CC, **Aleixo A**, **Nogueira AC**, **Miyaki CY**, **Cracraft J. 2012.** A palaeobiogeographic model for biotic diversification within Amazonia over the past three million years. *Proceedings. Biological sciences* **279:** 681–689.

Roberto IJ, **Loebmann D. 2016.** Composition, distribution patterns, and conservation priority areas for the herpetofauna of the state of Ceará, northeastern Brazil. *Salamandra* **52:** 134–152.

Ronquist F, **Teslenko M**, **van der Mark P**, **Ayres DL**, **Darling A**, **Höhna S**, **Larget B**, **Liu L**, **Suchard MA**, **Huelsenbeck JP. 2012.** MrBayes 3.2: efficient Bayesian phylogenetic inference and model choice across a large model space. *Systematic Biology* **61:** 539–542.

de Sá RO, **Tonini JFR**, **van Huss H**, **Long A**, **Cuddy T**, **Forlani MC**, **Peloso PLV**, **Zaher H**, **Haddad CFB. 2019.** Multiple connections between Amazonia and Atlantic Forest shaped the phylogenetic and morphological diversity of *Chiasmocleis* Mehely, 1904 (Anura: Microhylidae: Gastrophryninae). *Molecular Phylogenetics and Evolution* **130:** 198–210.

Sabaj MH. 2019. *Standard symbolic codes for institutional resource collections in herpetology and ichthyology: an online reference, version 7.1*. American Society of Ichthyologists and Herpetologists, USA. Available at https://asih.org/standard-symbolic-codes/about-symbolic-codes

Schneider JG. 1799. *Historia amphibiorium naturalis et literariae, fasciculus primus*. Jena: Friederich Frommann.

Silva JMC. 1995. Biogeography analysis of the South American Cerrado avifauna. *Steenstrupia* **21:** 49–67.

Silva JMC, **Bates JM. 2002.** Biogeographical patterns and conservation in the South American cerrado: a tropical savanna hotspot. *BioScience* **52:** 225–233.

Silva JMC, **Novaes FC**, **Oren DC. 2012.** Differentiation of *Xiphocolaptes* (Dendrocolaptidae) across the river Xingu, Brazilian Amazonia: recognition of a new phylogenetic species and biogeographic implications. *Bulletin of the British Ornithologists' Club* **122:** 185–194.

Silva LA, **Carvalho PS**, **Pereira EA**, **Fadel RM**, **Dantas SP**, **Brandão RA**, **Santana DJ. 2020.** Richness, diversity patterns, and taxonomic notes of amphibians from the Tocantins State. *Biota Neotropica* **20:** e20190383.

Silva SM, **Peterson AT**, **Carneiro L**, **Burlamaqui TCT**, **Ribas CC**, **Sousa-Neves T**, **Miranda LS**, **Fernandes AM**, **d'Horta FN**, **Araújo-Silva LE**, **Batista R**, **Bandeira CHMM**, **Dantas SM**, **Ferreira M**, **Martins DM**, **Oliveira J**, **Rocha TC**, **Sardelli CH**, **Thom G**, **Rêgo PS**, **Santos MP**, **Sequeira F**, **Vallinoto M**, **Aleixo A. 2019.** A dynamic continental moisture gradient drove Amazonian bird diversification. *Science Advances* **5:** e5752.

Smith BT, **McCormack JE**, **Cuervo AM**, **Hickerson MJ**, **Aleixo A**, **Cadena CD**, **Pérez-Emán J**, **Burney CW**, **Xie X**, **Harvey MG**, **Faircloth BC**, **Glenn TC**, **Derryberry EP**, **Prejean J**, **Fields S**, **Brumfield RT. 2014.** The drivers of tropical speciation. *Nature* **515:** 406–409.

Steindachner F. 1867. *Reise der österreichischen Fregatte Novara um die Erde in den Jahren 1857, 1858, 1859 unter den Bafehlen des Commodore B. von Wüllerstorf-Urbair, Zoologischer Theil, Amphibien*. Vienna: K. K. Hof- und Staatsdruckerei.

Sueur J, **Aubin T**, **Simonis C. 2008.** Seewave: a free modular tool for sound analysis and synthesis. *Bioacoustics* **18:** 213–226.

Turner T. 1998. Os Mebengokre Kayapó: história e mudança social, de comunidades autônomas para a coexistência

interétnica. In: Cunha, MCd, ed. *História dos índios no Brasil*, *2nd edn*. São Paulo: Companhia das Letras/Secretaria Municipal de Cultura/FAPESP, 311–338.

Wallace AR. 1852. The monkeys of the Amazon. *Proceedings of the Zoological Society of London* **20:** 107–110.

Wang X, **Edwards RL**, **Auler AS**, **Cheng H**, **Kong X**, **Wang Y**, **Cruz FW**, **Dorale JA**, **Chiang HW. 2017.** Hydroclimate changes across the Amazon lowlands over the past 45,000 years. *Nature* **541:** 204–207.

Watters JL, **Cummings ST**, **Flanagan RL**, **Siler CD. 2016.** Review of morphometric measurements used in anuran species descriptions and recommendations for a standardized approach. *Zootaxa* **4072:** 477–495.

Werneck FP, **Nogueira C**, **Colli GR**, **Sites JW**, **Costa GC. 2012.** Climatic stability in the Brazilian Cerrado: implications for biogeographical connections of South American savannas, species richness and conservation in a biodiversity hotspot. *Journal of Biogeography* **39:** 1695–1706.

SUPPORTING INFORMATION

Additional Supporting Information may be found in the online version of this article at the publisher's web-site:

Appendix S1. List of specimens morphologically examined (*Adenomera* spp.) in this study.
Appendix S2. GenBank accession numbers and locality data on voucher specimens included in the molecular analyses. New sequences are indicated in bold.
Appendix S3. Soundruler settings for the automated acoustic analysis and information on sound recordings (original file names) analysed in this study. See Supporting Information (Appendices S1–S2) for locality data of voucher specimens.
Figure S1. Phylogenetic relationships among lineages of the seven major clades of *Adenomera* based on molecular data. Within-lineage relationships collapsed. Numbers near the nodes indicate posterior probabilities (pp) and asterisks indicate full support (pp = 1.0). Branch scale is indicated in number of substitutions per site. Members of the A. *heyeri* clade are indicated by bold.
Figure S2. Time-calibrated phylogeny of *Adenomera* based on molecular data. Numbers above the nodes indicate posterior probabilities (pp) and asterisks indicate full support (pp = 1.0). Numbers below the nodes indicate mean divergence times (in Mya). Grey bars on the nodes indicate confidence intervals of divergence times. Branch scale is indicated in number of substitutions per site.